Fast Polygonal Approximation of Terrains and Height Fields

Michael Garland and Paul S. Heckbert

September 19, 1995

CMU-CS-95-181

School of Computer Science
Carnegie Mellon University
Pittsburgh, PA 15213

email: {garland,ph}@cs.cmu.edu
tech report & C++ code: http://www.cs.cmu.edu/~garland/scape

Abstract

Several algorithms for approximating terrains and other height fields using polygonal meshes are described, compared, and optimized. These algorithms take a height field as input, typically a rectangular grid of elevation data $H(x, y)$, and approximate it with a mesh of triangles, also known as a triangulated irregular network, or TIN. The algorithms attempt to minimize both the error and the number of triangles in the approximation. Applications include fast rendering of terrain data for flight simulation and fitting of surfaces to range data in computer vision. The methods can also be used to simplify multi-channel height fields such as textured terrains or planar color images.

The most successful method we examine is the *greedy insertion algorithm*. It begins with a simple triangulation of the domain and, on each pass, finds the input point with highest error in the current approximation and inserts it as a vertex in the triangulation. The mesh is updated either with Delaunay triangulation or with data-dependent triangulation. Most previously published variants of this algorithm had expected time cost of $O(mn)$ or $O(n \log m + m^2)$, where n is the number of points in the input height field and m is the number of vertices in the triangulation. Our optimized algorithm is faster, with an expected cost of $O((m+n) \log m)$. On current workstations, this allows one million point terrains to be simplified quite accurately in less than a minute. We are releasing a C++ implementation of our algorithm.

Contents

1.   Introduction

A *height field* is a set of height samples over a planar domain. Terrain data, a common type of height field, is used in many applications, including flight simulators, ground vehicle simulators, and in computer graphics for entertainment. Computer vision uses height fields to represent range data acquired by stereo and laser range finders. In all of these applications, an efficient data structure for representing and displaying the height field is desirable.

Our primary motivation is to render height field data rapidly and with high fidelity. Since almost all graphics hardware uses the polygon as the fundamental building block for object description, it seems natural to represent the terrain as a mesh of polygonal elements. The raw sample data can be trivially converted into polygons by placing edges between each pair of neighboring samples. However, for terrains of any significant size, rendering the full model is prohibitively expensive. For example, the 2,000,000 triangles in a $1,000 \times 1,000$ grid take about seven seconds to render on current graphics workstations, which can display roughly 10,000 triangles in real time (every 30th of a second). Even as the fastest graphics workstations speed up in coming years, typical workstations and personal computers will remain far slower. More fundamentally, the detail of the full model is highly redundant when it is viewed from a distance, and its use in such cases is unnecessary and wasteful. Many terrains have large, nearly planar regions which are well approximated by large polygons. Ideally, we would like to render models of arbitrary height fields with just enough detail for visual accuracy. Additionally, in systems which are highly constrained, we would like to use a less detailed model in order to conserve memory, disk space, or network bandwidth.

To render a height field quickly, we can use multiresolution modeling, preprocessing it to construct approximations of the surface at various levels of detail [3, 16]. When rendering the height field, we can choose an approximation with an appropriate level of detail and use it in place of the original. The various levels of detail can be combined into a hierarchical triangulation [6, 5].

In some applications, such as flight simulators, the speed of simplification is unimportant, because database preparation is done off-line, once, while rendering of the simplified terrain is done thousands of times. In more general computer graphics and computer animation applications, the scene being simplified might be changing many times per second, however, so a slow simplification method might be useless. Finding a simplification algorithm that is fast is therefore quite important

to us.

Our focus in this paper will be to generate simplified models of a height field from the original model. The simplified model should accurately approximate the original model, use as few triangles as possible, and the process of simplification should be as rapid as possible.

The remainder of this paper contains the following sections: We begin by stating the problem we are solving. Next we describe several methods for selecting the most important points of a height field. The core of the paper is the following section on the greedy insertion algorithm, where we begin with the basic algorithm, and through a progression of simple optimizations, speed it up dramatically. We explore the use of both Delaunay triangulation and data-dependent triangulation. The paper concludes with a discussion of empirical results, ideas for future work, and a summary.

1.1. Background

Our companion survey paper [17] contains a thorough review of surface simplification methods. To summarize, algorithms for polygonal simplification of surfaces can be categorized into six groups:

- *uniform grid methods,* which use a regular grid of samples in x and y;

- *hierarchical subdivision methods,* which are based on quadtree, k-d tree, and hierarchical triangulations;

- one pass *feature methods,* which select a set of important "feature" points (such as peaks, pits, ridges, and valleys) in one pass and use them as the vertex set for triangulation;

- multi-pass *refinement methods* which start with a minimal approximation and use multiple passes of point selection and retriangulation to build up the final triangulation;

- multi-pass *decimation methods,* which begin with a triangulation of all of the input points and iteratively delete vertices from the triangulation, gradually simplifying the approximation; and

- other methods, including adjustment techniques, optimization-based methods, and optimal methods.

The latter four simplification methods typically employ general triangulations that are neither uniform nor hierarchical. Two such general triangulation methods are Delaunay triangulation and data-dependent triangulation.

Delaunay triangulation is a purely two-dimensional method; it uses only the xy projections of the input points. It finds a triangulation that maximizes the minimum angle of all triangles, among all triangulations of a given point set [13, 21]. This helps to minimize the occurrence of very thin *sliver* triangles. *Data-dependent triangulation*, in contrast, uses the heights of points in addition to their x and y coordinates [8, 31]. It can achieve lower error approximations than Delaunay triangulation, but it generates more slivers.

2. Statement of Problem and Approach

We assume that a discrete two-dimensional set of samples H of some underlying surface is provided. This is most naturally represented as a discrete function where $H(x, y) = z$ means
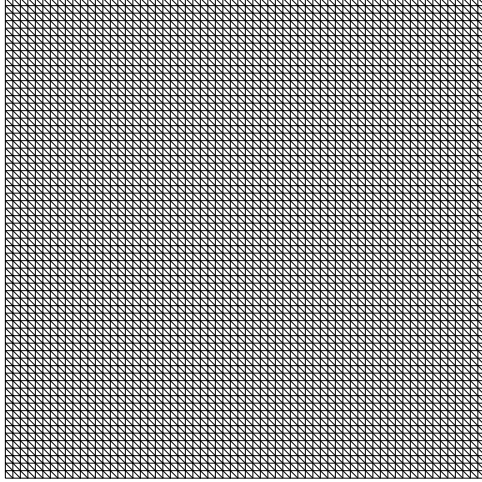
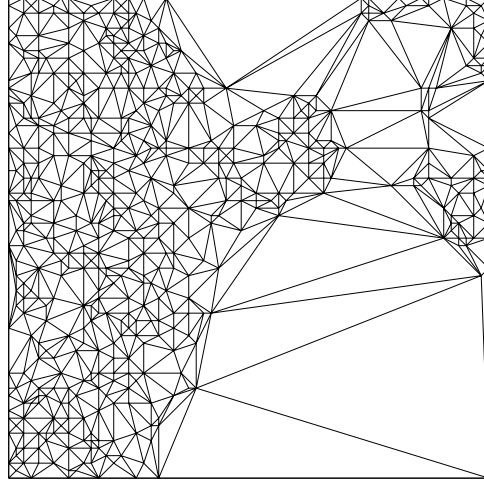Figure 1: Uniform grid triangulation of 65×65 height field H.

Figure 2: A triangulation $\mathcal{T}S$ using 512 vertices that approximates H; an example of a triangulated irregular network.

that the point (x, y, z) lies on the actual surface. We will assume that this discrete sampling is performed on a rectangular grid at integer coordinates, but the methods we will describe are easily generalized to scattered data points. Finally, we assume that the surface will be reconstructed from H by triangulating its points; abstractly, the reconstruction operator $\mathcal{T}$ maps a function defined over a scattered set of points in a continuous domain (a function such as H) to a function defined at every point in the domain. It accomplishes this by building a triangulation of the sample points and using this triangulated surface to give values to all points which are not part of the grid. If S is some subset of input points, then $\mathcal{T}S$ is the reconstructed surface, and $(\mathcal{T}S)(x, y)$ is the value of the surface at point (x, y). Such a triangulated approximation is often referred to as a *triangulated irregular network*, or TIN. See Figures 1 and 2.

Our goal is to find a subset S of H which, when triangulated, approximates H as accurately as possible using as few points as possible, and to compute the triangulation as quickly as possible. This is thus an optimization problem. The number of input points in H is n. The number of points in the subset S is m, and consequently the number of vertices in the triangulation is also m.

2.1. Approach

The principal class of algorithms that we explore in this paper are *refinement methods*. We do not use uniform grids or hierarchical subdivision because they cannot deliver the quality that we require, and we will not pursue brute force optimization methods because they are too slow. Refinement methods are multi-pass algorithms that begin with an initial approximation and iteratively add new points as vertices in the triangulation. The process of refinement continues until some specific goal is achieved, usually reaching a desired error threshold or exhausting a point budget. In order to choose which points to add to the approximation, refinement methods rank the available input points using some *importance measure*.

In exploring importance measures, we reject those that make use of implicit knowledge about the nature of terrains, such as the existence of ridge lines. We would like our algorithms to apply to general height fields, where assumptions that are valid for terrains might fail. Even if we were to constrain ourselves to terrains alone, we are not aware of conclusive evidence suggesting that high fidelity results (as measured by an objective L_2 or L_∞ metric[1]) require high level knowledge of terrains.

3.   Importance Measures

Within the basic framework outlined above, the key to good simplification lies in the choice of a good point importance measure. But what criteria should be used to judge such a measure? Ultimately, the final judgement must depend upon the quality of the results it produces. With this in mind, we suggest that a good measure should be simple and fast, it should produce good results on arbitrary height fields, and it should use only local information. The requirement that a measure be simple and fast is easy to justify; since we will be simplifying detailed terrains and height fields, the importance measure will be evaluated many times. Consequently, any cost inherent in the importance measure will be magnified many times due to its repetition. We also demand that the measure apply equally well to all height fields whether they are terrains, colored textures, or other semi-continuous functions. This becomes increasingly important for the simplification of height fields with color texture or other material properties, which we will discuss later. Measures which depend on characteristics peculiar to terrains or any other specific kind of height field, are unacceptable to us. Finally, the importance measure should use only local information. This requirement is necessary to support some significant optimizations in the algorithm's running time.

We explored four categories of importance measures: local error, curvature, global error, and products of selected other measures. We briefly discuss each of these below.

3.1.   Local Error Measure

The first measure which we explored is simple vertical error. The importance of a point (x, y) is measured as the difference between the actual function and the interpolated approximation at that point (i.e. $|H(x, y) - (\mathcal{T}S)(x, y)|$). This difference is a measure of local error. Intuitively, we would expect that eliminating such local errors would yield high quality approximations, and it generally does. This measure also meets the other criteria suggested earlier: it is simple, fast, and uses only local information.

3.2.   Curvature Measure

The piecewise-linear reconstruction effected by $\mathcal{T}$ approximates nearly planar functions well, but does more poorly on curved surfaces. However, in everyday life, peaks, pits, ridges, and valleys, which have high curvature, are visually significant. These observations suggest that we try curvature as a measure of importance.

---

[1]In this paper, we use the following error metrics: We define the L_2 error between two n-vectors $\mathbf{u}$ and $\mathbf{v}$ as $||\mathbf{u} - \mathbf{v}||_2 = \left[\sum_{i=1}^{n} (u_i - v_i)^2 \right]^{1/2}$. The L_∞ error, also called the *maximum error*, is $||\mathbf{u} - \mathbf{v}||_\infty = \max_{i=1}^{n} |u_i - v_i|$. We define the *squared error* to be the square of the L_2 error, and the *root mean square* or RMS error to be the L_2 error divided by $\sqrt{n}$. Optimization with respect to the L_2 and L_∞ metrics are called *least squares* and *minimax* optimization, and we call such solutions L_2–*optimal* and L_∞–*optimal*, respectively.
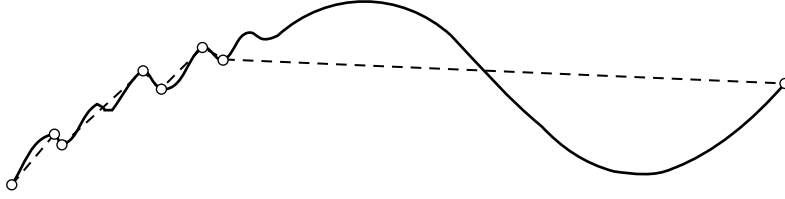
Figure 3: Cross section of a hypothetical terrain that is small-scale rough and large-scale smooth on the left, but small-scale smooth and large-scale rough on the right. An importance measure based on local curvature measures would generate a poor approximation like the one shown dashed (selected features marked with dots).

In one dimension, $|H''|$ is a good curvature measure. Since H is a discrete function, we estimate its derivatives numerically using central differences. Note that this measure of importance is independent of the current approximation; it is essentially a *feature method* [17]. Hence, it lends itself to a one pass approach: compute values for $|H''|$ at all points and select the m points with the highest values. However, the method is over-sensitive to high frequency variations. A series of extreme and rapid fluctuations, such as a saw tooth, which are relatively small in scale, are not visually significant when viewed at a distance; however, each fluctuation would seem like an important feature and would therefore be allocated points which might be better used elsewhere (Figure 3). In order to circumvent this problem, we performed an initial smoothing pass with a Gaussian filter and computed derivatives on this smoothed function in order to estimate curvature at various scales (points were still selected from the original unsmoothed version). The filtering pass removed small fluctuations but left large features intact [24].

This scheme appeared promising in several respects. First, the algorithm was much faster than iterative refinement techniques because the final approximation can be constructed in a single pass. Second, by increasing the standard deviation of the Gaussian kernel, the smoothing preprocess could smooth away progressively larger details. Finally, the measure satisfied the criteria which we have suggested above. Unfortunately, when tested on curve simplification problems, the resulting approximations were not of comparable quality to those produced by the local error measure.

Because the curvature measure was inferior in one dimension, we did not test it in two dimensions. We will describe how it could be generalized to two dimensions, however. One might think that the Laplacian, $\partial^2 H/\partial x^2 + \partial^2 H/\partial y^2$, would be a good measure of curvature for functions of two variables. The Laplacian is a poor measure, however, because it sums the curvatures in the x and y directions, and these could cancel, as at a saddle. Consider $H(x,y) = ax^2 - ay^2$, for any a, for example. A better measure is the sum of the squares of the principal curvatures [37], which can be computed as the square of the Frobenius norm of the Hessian matrix (known as the second fundamental form in differential geometry [36]): $(\partial^2 H/\partial x^2)^2 + 2(\partial^2 H/\partial x\partial y)^2 + (\partial^2 H/\partial y^2)^2$. Similar curvature measures have been explored for approximation purposes by others [25, 33, 32]. We do not expect such measures to yield high quality approximations, however, since the curvature approach did not work well for curves.

3.3. Global Error Measure

We next tested the global error, or sum of errors over all points, as an importance measure. We expected that this "more intelligent" error measure would yield higher quality results than the local error measure, but at a penalty in speed.

5

At every point, we compute the global resultant error of a new approximation formed by adding that point to the current approximation, measured as $\sum_{x,y} |H(x,y) - (\mathcal{T}S)(x,y)|$. Then we merely select the point that produces the smallest global error. This approach is similar to one move look-ahead in game playing algorithms, or hill climbing. Compared to the local error measure, instead of simply assuming that the addition of points of high local error will in fact decrease the global error, it chooses the point which actually minimizes the global error. This measure violates one of our stated criteria; it is not local. However, it seemed that this approach might give better results than the previous measure.

The algorithm would seem prohibitively expensive, but it is not, at least in one dimension. If you are willing to sacrifice $O(n)$ space and time to precompute several partial sum arrays, the global error resulting after the introduction of a point can be computed in constant time.

When tested on curves, the global error measure yielded poor results. This was surprising, since we had expected it to yield better results than the simpler local error measure. This is simply an instance of a standard problem with hill climbing optimization methods: they are too short sighted. It is often necessary to make several "bad" moves in the short term to achieve long term success. In our case, accurately fitting a particular feature might require the addition of at least two points. It is quite possible that introducing the first point will introduce significant error which will be eradicated by introducing the second point. The global error measure is too conservative; it is too concerned with the immediate consequences of inserting any particular point and not knowledgeable enough to see possible future benefits from this action. While it might be possible to fix this behavior using a standard technique such as simulated annealing, this would only further increase the cost of this already expensive algorithm. It appears unlikely that this high expense would produce correspondingly better results than those achieved using the simpler local error measure.

A second problem with the global error measure is that there does not appear to be a generalization of the partial sum trick that would permit errors over triangles to be computed in constant time.

3.4. Product Measures

The last approach to measuring importance which we explored was another attempt to improve upon the local error measure. One would think that this could be improved upon using a more informed heuristic function. We tested the performance of a set of related measures formed by the product of several simpler measures[2]. The method we used was to combine one or more of the importance measures given above with some bias measures. Two examples of bias measures are: absolute height, and the ratio of the number of unselected points in a region to the number of points remaining to be selected. Using these product measures, we were able to achieve results which were only slightly poorer than those produced by the local error measure. However, product measures are more complex, and hence more expensive, than any of the measures discussed so far with the exception of global error. Thus, the resulting algorithm was significantly slower.

---

[2]We use products rather than sums because the units of measure of the constituent terms are generally unrelated. Thus, simple summation does not yield meaningful information.

3.5. Decimation Algorithms

We next investigated decimation variants of two of these measures. The curvature measure has no decimation variant since it is not iterative, and decimation with the local error measure is essentially the same as Lee's drop heuristic algorithm [22].

We tested decimation variants of the global error measure and the product measure on curves. The results were interesting, but ultimately poorer than other methods. We found that the global error measure produced more accurate approximations when used in a decimation algorithm than in a refinement algorithm. Proceeding from a detailed approximation to a cruder one ameliorated the problems of the global error measure; in a decimation algorithm there seems to be less need to look several moves ahead. Thus, if the algorithm simply removes the point whose absence adds the smallest error to the approximation, this will lead to a good approximation in most cases. Product measures incorporating the global error measure also performed better in a decimation algorithm, but the performance of other product measures was essentially unchanged. However, the results of these decimation algorithms were still slightly less accurate than those produced by the local error measure.

3.6. Conclusions from Importance Measure Experiments

Importance measures which make no reference to the approximation (such as most feature methods) were not very successful in our experiments. A fundamental flaw of most such methods is that they give no guarantee about the accuracy of their approximations. The cause of this low quality seems to be the independence and locality of decisions made by most of these algorithms.

A terrain that is rough at a small scale but nearly planar at a large scale (e.g., a city) will have many high-importance points, while a terrain that is smooth at a small scale and rough at a large scale (e.g., rolling hills) will have few. If these two terrain types are both present in a single dataset, too many features will be devoted to regions of the first type and too few to the latter, leading to poor simplification, as shown in Figure 3. The methods behave poorly in the presence of noisy height data for similar reasons.

After empirical comparison of results from the above methods, we settled on the local error measure for iterative refinement. We found that it was the simplest to implement, produced more accurate results than any of our alternatives, and was faster than all but the curvature measure. We will demonstrate in the following sections that this algorithm is easily generalized to other simplification problems, and that it can be fast.

4. Greedy Insertion

We call refinement algorithms that insert the point(s) of highest error on each pass *greedy insertion* algorithms, "greedy" because they make irrevocable decisions as they go [4], and "insertion" because on each pass they insert one or more vertices into the triangulation. Methods that insert a single point in each pass we call *sequential greedy insertion* and methods that insert multiple points in parallel on each pass we call *parallel greedy insertion*. The words "sequential" and "parallel" here refer to the selection and re-evaluation process, not to the architecture of the machine. Many variations on the greedy insertion algorithm have been explored over the years; apparently the algorithm has been reinvented many times [10, 7, 18, 31, 28, 11, 30].

We now explore four variants of the sequential greedy insertion algorithm. Our first method,

algorithm I, is a brute force implementation of sequential greedy insertion with Delaunay triangulation. This algorithm is quite slow, so we present two optimizations. Algorithm II exploits the locality of changes to the triangulation to eliminate redundant recalculation of error, and algorithm III goes further, employing better data structures to speed selection of the point of highest error. The result is an algorithm that computes high quality approximations very rapidly. Next, we take this algorithm and replace Delaunay triangulation with data-dependent triangulation, yielding algorithm IV, which generates slightly higher quality approximations than algorithm III.

4.1. Basic Algorithm

We begin with some basic functions that query the Delaunay mesh[3] and perform incremental Delaunay triangulation. The routine MESH_INSERT locates the triangle containing a given point, splits the triangle into three, and then recursively checks each of the outer edges of these triangles, flipping them if necessary to maintain a Delaunay triangulation (Figure 4) [13].

MESH_INSERT(*Point p*)*:* Insert p as a vertex in the Delaunay mesh

MESH_LOCATE(*Point p*)*:* Find the triangle in the mesh containing point p

LOCATE_AND_INTERPOLATE(*Point p*)*:* Locate the triangle containing point p and interpolate there

INSERT(*Point p*):
  mark p as used
  MESH_INSERT(p)

ERROR(*Point p*):
  % Returns the error at a point (our importance measure)
  return $|H(p) - $ LOCATE_AND_INTERPOLATE$(p)|$

The heart of the algorithm is sequential greedy insertion, much as described in earlier work [7, 31, 11]. It is simple and unoptimized. We build an initial approximation of two triangles using the corner points of H. Then we repeatedly scan the unused points to find the one with the largest error and call INSERT to add it to the current approximation. The conditions for termination are stated abstractly as a function GOAL_MET; they would typically be based on the number of points selected, the maximum (L_∞) error of the approximation, or the squared (L_2) error of the approximation.

---

[3]The terms "mesh" and "triangulation" are used synonymously henceforth.

Algorithm I:

GREEDY_INSERT():
    initialize mesh to two triangles with the height field grid corners as vertices
    while not GOAL_MET() do
        $best \leftarrow$ nil
        $maxerr \leftarrow 0$
        forall input points p do
          $err \leftarrow$ ERROR(p)
         if $err > maxerr$ then
            $maxerr \leftarrow err$
            $best \leftarrow p$
        INSERT($best$)

4.1.1. Cost Analysis of Algorithm I

Let us consider the time complexity of this algorithm. For the purposes of analysis, we will assume that our input grid has a total of n points and that m points will be selected for the approximation. For now, suppose that L is the time to locate one point in the Delaunay mesh and I is the time to insert a vertex in the mesh. Let i be the pass number.

Within each pass, we classify costs into three categories:

selection to pick the best point,

insertion to insert a vertex into the mesh, and

recalculation to recalculate errors at grid points.

To find the best point, we scan through $O(n)$ points[4] performing comparisons. We perform a single mesh insertion which has cost I. Finally, for every unused point, of which there are $O(n-i)=O(n)$, we must also perform a recalculation. Recalculation involves a mesh *location* query to find that point's containing triangle and an *interpolation* to find the value of the approximation at that point. The cost for each location is L and the cost for each interpolation is $O(1)$. The cost for location might increase with successive passes, since the number of vertices in the mesh at the beginning of pass i is $i+4$. So the cost of recalculation on each pass is $O(nL)$.

Worst Case Cost. The cost of location, L, and the cost of insertion, I, are mesh-dependent. A planar triangulation with v vertices total, v_b of them on the boundary, will have $3v-v_b-3$ edges and $2v-v_b-2$ triangles [21]. Typically, $v_b=O(\sqrt{v})$, in which case the number of edges is approximately $3v$ and the number of triangles is about $2v$, but in any case, the number of edges and the number of triangles are each $O(v)$.

For point location, we can use the simple "walking method" due to Guibas-Stolfi, Green-Sibson, and Lawson [13, p. 121], [12], [21]. This algorithm starts on an edge of the mesh, and walks through the mesh toward the target point until it arrives at the target. If it were to start in a very unlucky spot, on a mesh with $i+4$ vertices, it might have to walk across almost all $O(i)$ edges. Mesh insertion involves locating the containing triangle of a point, inserting a new vertex there, and potentially flipping some edges. At worst, the location will require $O(i)$ time, and $O(i)$ edges

---

[4]It would require too much space to represent the set of input points explicitly. Therefore we assume that it is represented as a Boolean array recording whether a particular entry has been used or not. Thus, the entire array H must be scanned in order to find the unused points.

will need to be flipped. So mesh location and insertion can require time linear in the number of points in the mesh, and $L = I = O(i)$.

Thus, in the worst case, the costs per pass for algorithm I are: $O(n)$ for selection, $O(i)$ for insertion, and $O(in)$ for recalculation. The asymptotically dominant term is recalculation, so the total worst case cost is $\sum_{i=1}^{m} O(in) = O(m^2 n)$.

Expected Case Cost. Fortunately, the worst case behavior is very unlikely. In practice, it is the expected cost behavior which we observe. So the expected cost is a much more important measure of the practical speed of the algorithm.

The expected cost for random access location queries in a Delaunay mesh with v vertices for typical point distributions is only $L = O(\sqrt{v})$ [13, 14]. However, if successive location queries are close together, then the location procedure can start its search at the triangle returned by the previous call so that very few steps will be needed to find the next target point. In this situation, the expected cost of location is $L = O(1)$ [13].

In the algorithm above, point location queries almost always occur near one another. All but a few of them are made in the process of scanning the unused points. Since this scanning proceeds across each row in order, successively scanned points are almost always nearby and are usually direct neighbors. Of course, it is possible to construct meshes in which both insertion and location will have linear cost. We cannot guarantee that this will never happen, but the conditions under which this behavior might arise are very uncommon. In the course of our experiments, this degeneracy has never yet occurred in practice. So the expected cost of location during recalculation is $L = O(1)$.

Insertion involves a location query that usually does not exhibit as much spatial coherence as location queries due to recalculation, so its expected cost in this context is $L = O(\sqrt{i})$. The other costs of insertion are due to edge flips. On average, the number of edge flips is constant, and each takes constant time, with Delaunay triangulation, so the expected cost for insertions is $I = O(\sqrt{i})$.

Assuming $L = O(1)$ and $I = O(\sqrt{i})$ in the expected case, the costs per pass for algorithm I are: $O(n)$ for selection, $O(\sqrt{i})$ for insertion, and $O(n)$ for recalculation. The asymptotically dominant terms are selection and recalculation, so the total expected case cost is $\sum_{i=1}^{m} O(n) = O(mn)$.

4.2. Faster Recalculation

The algorithm above yields high quality results. However, even our expected time complexity estimate of $O(mn)$ is expensive, and the worst case complexity of $O(m^2 n)$ is exorbitant. Fortunately, we can improve upon our original naive algorithm considerably by exploiting the locality of the changes to the approximation during incremental Delaunay triangulation.

4.2.1. Delaunay Triangulation

The incremental Delaunay triangulation algorithm is illustrated in Figure 4, and works as follows [13, 21]: To insert a vertex A, locate its containing triangle, or, if it lies on an edge, delete that edge and find its containing quadrilateral. Add "spoke" edges from A to the vertices of this containing polygon. All perimeter edges of the containing polygon are suspect and their validity must be checked. An edge is valid iff it passes the circle test: if A lies outside the circumcircle of the triangle that is on the opposite side of the edge from A. All invalid edges must be swapped with the other diagonal of the quadrilateral containing them, at which point the containing polygon acquires two new suspect edges. The process continues until no suspect edges remain. The resulting

triangulation is Delaunay.

4.2.2. Exploiting Locality of Changes

After insertion, the point inserted will have edges emanating from it to the corners of a surrounding polygon [13]. This polygon defines the area in which the triangulation has been altered, and hence, it defines the area in which the approximation has changed (see Figure 4c). We call this polygon the *update region*. Such coherence permits our first significant optimization: we will cache the values of ERROR and recompute them only within the update region. We define an array *Cache* containing error values indexed by the set of input points. We must make only three small modifications to our earlier algorithm: alter GREEDY_INSERT to initialize *Cache*, change INSERT to update values in *Cache* that have changed due to insertion, and make the main loop of GREEDY_INSERT look up values in *Cache* rather than calling ERROR directly. We can visit all grid points in the update region by scan converting the triangles surrounding the inserted point. Or, even simpler, we can overestimate the update region by computing the bounding box of these triangles. The modified portions of the algorithm now look like:

Algorithm II:

INSERT(*Point p*):
   mark p as used
   MESH_INSERT(p)
   forall points q inside the triangles incident on p do
      Cache[q] ← ERROR(q)

GREEDY_INSERT():
   initialize mesh to two triangles with the height field grid corners as vertices
   forall input points p do
      Cache[p] ← ERROR(p)
   while not GOAL_MET() do
      best ← nil
      maxerr ← 0
      forall input points p do
         err ← *Cache*[p]
        if *err* > *maxerr* then
           maxerr ← *err*
           best ← p
      INSERT(*best*)

4.2.3. Cost Analysis of Algorithm II

As with the original algorithm, the three categories of expense remain: selection, insertion, and recalculation (the latter involving both location and interpolation). The costs for selection and insertion are unchanged, but we now perform far fewer recalculations in most cases. Let A be the area of the update region on pass i. We are still doing a location query for each recalculated point, so the cost per pass for recalculation is $O(AL)$ for location and $O(A)$ for interpolation.

Worst Case Cost. In the worst case, the area to be updated shrinks by only a constant amount on each pass, so $A = O(n - i)$. While this is only true of pathological cases, it is still a possibility. In this case, the cost for recalculation is the same as in the original algorithm, and this remains the dominant cost, so the worst case complexity for algorithm II is unchanged at $O(m^2 n)$.
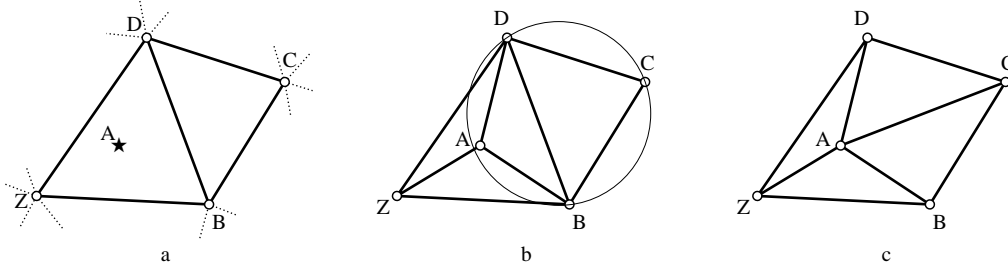
Figure 4: Delaunay triangulation: a) Point A is about to be inserted. Spoke edges from A to the containing polygon ZBD are added. b) The quadrilateral around suspect edge BD is checked using the circle test. The circumcircle of BCD contains A, so edge BD is invalid. c) After swapping edge BD for AC, edges BC and CD become suspect. The polygon ZBCD is the only area of the mesh that has changed.

Expected Case Cost. For most surfaces, the update region has expected area $A = O(n/i)$, since n points divided among approximately $2i$ triangles gives an average area of $O(n/i)$. As discussed in the analysis of the original algorithm, the expected costs per pass for location and insertion are $L = O(1)$ and $I = O(\sqrt{i})$, respectively. The costs per pass for algorithm II are thus: $O(n)$ for selection, $O(\sqrt{i})$ for insertion, and $O(n/i)$ for recalculation. The asymptotically dominant term is now selection, recalculation having become less expensive, so the total expected case cost is also unchanged: $\sum_{i=1}^{m} O(in) = O(mn)$.

If we consider only the asymptotic time complexities, this new algorithm appears no faster than the original naive version, but that is not true in practice. Firstly, the worst case behavior for algorithm II is even more unlikely than it was for algorithm I. Secondly, asymptotic complexities can hide significant constants. In the expected case, the constant factors have decreased significantly. In particular, in algorithm I both recalculation and selection had an expected per-pass cost of $O(n)$. In algorithm II, only selection has an expected cost of $O(n)$ per pass; the expected cost for recalculation per pass has dropped to $O(n/i)$. The constant cost factor for recalculation is much higher than that for selection, so recalculation is the dominant cost of algorithm II in practice. Since recalculation has a total expected cost[5] of only $\sum_{i=1}^{m} O(n/i) = O(n \log m)$, our new algorithm should be much faster than the original. This conclusion is supported by empirical timing data presented later.

4.3. Faster Selection

This leads us to the next avenue of optimization. The asymptotic expected cost of our algorithm is being held up by the cost of scanning the entire input grid to select the best point. This could be done more quickly with a heap [4] or other fast priority queue. We define the *candidate point* of a triangle to be the grid point within the triangle that has the highest error in the current approximation. Each triangle can have zero or one candidate point. Most triangles have one candidate, but if the maximum error inside the triangle is negligible, or there are no input points inside the triangle, then the triangle has none. Candidates are maintained in a heap keyed on their errors. During each pass, we simply extract the best candidate from the top of the heap.

After selection, a second expensive activity in algorithm II is recalculation. Even though it

---

[5]Recall that $\sum_{i=1}^{m} 1/i = O(\log m)$ and $\sum_{i=1}^{m} \log i = O(m \log m)$.

doesn't dominate the expected case complexity analysis, recalculation is very expensive in practical terms. So far, the ERROR function used for recalculation has done a point location to find the enclosing triangle and an interpolation within the triangle. In our implementations of algorithms I and II, interpolation is done by computing the plane defined by the three corners of the triangle and evaluating this plane equation at the specified point. All this is done each time a point's error is recalculated. Recalculation can be sped up in two ways. First, we can eliminate point location altogether, by recording with each candidate a pointer to its containing triangle. Second, we can speed up interpolation by a constant factor by precomputing plane equations and caching them with the triangle. As we scan convert a triangle, we track the best candidate seen so far.

4.3.1.   Data Structures

Since the data structures are becoming more complex, we will describe them more precisely. Algorithm III, to be presented shortly, has the following primary data structures: planes, height fields, triangulations, and heaps. The plane data structure is little more than three coefficients a, b, and c for a plane equation $H = ax + by + c$.

The height field consists of a rectangular array of points, each of which contains a height value $H(x, y)$, and a bit to record if the input point has been used by the triangulation.

For the triangulation, we use a slight modification to Guibas and Stolfi's quad-edge data structure [13], consisting of 2-D points, directed edges, and triangles in an interconnected graph. Each edge points to neighboring edges and to a neighboring triangle. Triangles contain a pointer to one of their edges, information about their candidate (its position *candpos* and a pointer into the heap *heapptr*) and the error over the triangle *err*. The pointer into the heap allows candidates to be updated quickly and also allows fast retrieval of the candidate's error.

The heap is a binary tree of records, each consisting of the candidate's error and a pointer to the triangle to which the candidate belongs. The latter information allows point location to be done in constant time after the candidate of highest error is extracted from the heap.

Note that depending on the details of the point inclusion test used or the scan conversion algorithm, points on an edge might be considered to be "inside" both of the adjacent triangles, in which case neighboring triangles might have identical candidates (see Figure 11). To avoid multiple visits to edge points, one could use rational arithmetic during scan conversion. A careful scan converter can also insure that vertices of the triangles are never visited. This can remove the need for the Boolean array of "used bits", provided that they are not needed for any other purposes. In our experience, this is a minor detail; the algorithm will work whether edge points are multiply counted or not.

4.4.   Optimized Delaunay Greedy Insertion

With selection speeded by a heap, location eliminated, and faster interpolation, our optimized algorithm is now:

Algorithm III: Delaunay Greedy Insertion:

HeapNode Heap_Change(*HeapNode h,* float *key, Triangle T*):
  % Set the key for heap node *h* to *key*, set its triangle pointer to *T*, and adjust heap.
  % Return (possibly new) heap node.
  if $h \neq$ nil then
    if *key* > 0 then
      Heap_Update(*h, key*) % update existing heap node
    else
      Heap_Delete(*h*)   % delete obsolete heap node
      return nil
  else
    if *key* > 0 then
      return Heap_Insert(*key, T*) % insert new heap node
  return *h*

Scan_Triangle(*Triangle T*):
  plane ← Find_Triangle_Plane(*T*)
  best ← nil
  maxerr ← 0
  forall points *p* inside triangle *T* do
    err ← $|H(p) -$ Interpolate_To_Plane(*p, plane*)$|$
    if *err* > *maxerr* then
      maxerr ← *err*
      best ← *p*
  T.heapptr ← Heap_Change(*T.heapptr, maxerr, T*)
  T.candpos ← *best*

Mesh_Insert(*Point p, Triangle T*): Insert a new vertex in triangle *T*, and update the Delaunay mesh

Insert(*Point p, Triangle T*):
  mark *p* as used
  Mesh_Insert(*p, T*)   % incremental Delaunay triangulation
  forall triangles *U* adjacent to *p* do
    Scan_Triangle(*U*)

Greedy_Insert():
  initialize mesh to two triangles with the height field grid corners as vertices
  forall initial triangles *T* do
    Scan_Triangle(*T*)
  while not Goal_Met() do
    T ← Heap_Delete_Max()
    Insert(*T.candpos, T*)

4.4.1. Cost Analysis of Algorithm III

Asymptotically, the most significant speedup relative to algorithm II is faster selection. In practice, optimization of interpolation is probably equally important.

In the new algorithm, time for selection is spent in three places: heap insertion, heap extraction, and heap updates. Clearly, the growth of the heap per pass is bounded by a constant, the net growth in the number of triangles, which is 2. However, the heap does not always grow this fast. In particular, as triangles become so small or so well fit to the height field as to have no candidate

Algorithm	Selection	Insertion	Recalculation
I	$O(n)$	$O(i)$	$O(in)$
II	$O(n)$	$O(i)$	$O(in)$
III or IV	$O(\log i)$	$O(i)$	$O(n)$

Table 1: Worst case cost per pass, for pass i

points, they will be removed from the heap. The heap grows initially at 2 items per pass, and as refinement proceeds, the growth slows and eventually the heap will begin to shrink. Typically, the approximations that we wish to produce are much smaller than the original height fields. Consequently, the algorithm will rarely realize any significant benefit from shrinking heap sizes. We will simply assume that the size of the heap is $O(i)$, and thus, that individual heap operations require $O(\log i)$ time in an amortized sense.

The number of changes made to the heap per pass is 3 plus the number of edge flips performed during mesh insertion. We assume that this is a small constant number. This is both reasonable and empirically confirmed on our sample data; in practice, the number of calls over time to HEAP_CHANGE per pass is roughly 3–5. Given this assumption, the total heap cost, and hence selection cost, is $O(\log i)$ per pass.

The other two tasks, insertion and recalculation, are also cheaper now, since neither performs locations. The cost of recalculation has dropped from $O(AL)$ to $O(A)$.

Worst Case Time Cost. In the worst case, the insertion time is $I = O(i)$ and the update area is $A = O(n)$, so the costs per pass for algorithm III are: $O(\log i)$ for selection, $O(i)$ for insertion, and $O(n)$ for recalculation. The asymptotically dominant term is recalculation, as before, but it is much smaller now; the total worst case cost is only $\sum_{i=1}^{m} O(n) = O(mn)$.

Expected Case Time Cost. In the expected case, the cost of insertion is $I = O(1)$ and the size of the update region is $A = O(n/i)$. Insertion has become very cheap because it no longer does a location query, and in the expected case we perform only a constant number of edge flips. The costs per pass for algorithm III are thus: $O(\log i)$ for selection, $O(1)$ for insertion, and $O(n/i)$ for recalculation. The selection cost grows as the passes progress, while the recalculation cost shrinks. These two are the dominant terms. The total expected case cost for algorithm III is thus: $\sum_{i=1}^{m} O(\log i + n/i) = O((m+n)\log m)$, which is much lower than that for the preceding two algorithms.

Memory Cost. Algorithm III uses memory for three main purposes: the height field, the mesh, and the heap. The height field uses space proportional to the number of grid points n, and the mesh and heap use space proportional to the number of vertices in the mesh, m. Asymptotically, the memory cost is thus $O(m+n)$. See section 5.2 for a detailed analysis of our current implementation.

Cost Summary. The complexity figures for the three algorithms presented are summarized in Tables 1, 2, and 3. Tables 1 and 2 detail the worst and expected costs per pass, respectively. Table 3 provides a summary of the total worst case and expected time complexity for each of the algorithms.

Algorithm	Selection	Insertion	Recalculation
I	$O(n)$	$O(\sqrt{i})$	$O(n)$
II	$O(n)$	$O(\sqrt{i})$	$O(n/i)$
III or IV	$O(\log i)$	$O(1)$	$O(n/i)$

Table 2: Expected case cost per pass, for pass i

Algorithm	Worst Case	Expected
I	$O(m^2n)$	$O(mn)$
II	$O(m^2n)$	$O(mn)$
III or IV	$O(mn)$	$O((m+n)\log m)$

Table 3: Time complexity summary

4.5.   Data-Dependent Triangulation

The previous algorithms employ Delaunay triangulation, which uses only two-dimensional (xy) information, and strives to create well-shaped triangles in 2-D. Delaunay triangulation ignores the heights of vertices and makes no use of the height field being approximated. More accurate approximation is possible using data-dependent triangulation, where the topology of the triangulation is chosen based on the three-dimensional fit of the approximating surface to the input points.

Data-dependent variants of the greedy insertion algorithms described can be created by replacing Delaunay triangulation with data-dependent triangulation, as discussed by Rippa and Hamann-Chen [31, 15]. The vertex to insert in the triangulation on each pass is chosen as before, but the triangulation is done differently.

The incremental Delaunay triangulation algorithm of section 4.2.1 tested suspect edges using a purely two-dimensional geometric test involving circumcircles. A generalization of this approach, Lawson's local optimization procedure [21], uses other tests. For data-dependent triangulation, instead of checking the validity of an edge with the circle test, the rule we adopt is that an edge is swapped if the change decreases the error of the approximation. We defer the definition of "error" until later. When used with the circle test, the local optimization procedure finds a global optimum, the Delaunay triangulation, but when used with more general tests, it is only guaranteed to find a local optimum.

Figure 5 illustrates the data-dependent triangulation algorithm. Figure 5a: suppose that point A has the highest error of all candidates. It will be the next vertex inserted in the triangulation. Figure 5b: spokes are added connecting it to the containing polygon (a triangle, if A falls inside a triangle; a quadrilateral, if A falls on an edge). Each edge of the containing polygon is suspect, and must be tested. In some cases, the quadrilateral containing the edge will be concave, and can only be triangulated one way, but in most cases, the quadrilateral will be convex, and the other diagonal must be tested to see if it yields lower error.

The most straightforward way to test validity of an edge BD would be the following recursive procedure: Test both ways of triangulating the quadrilateral ABCD containing the edge. If edge BD yields lower global error (Figure 5c), then no new suspect edges are added, and we stop recursing.
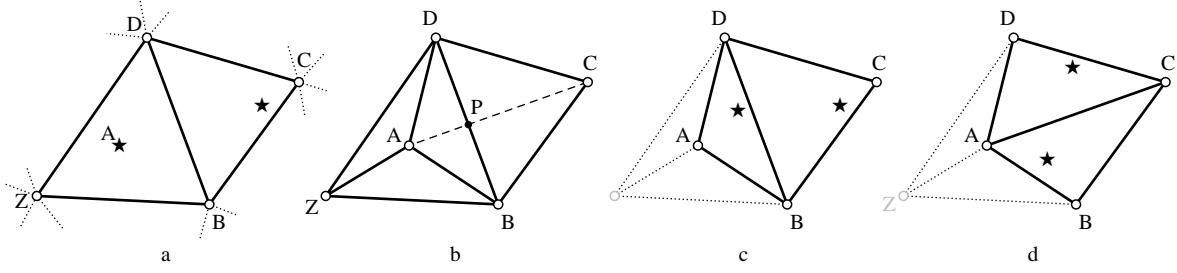
16

Figure 5: Data-dependent triangulation. a) Point A, the candidate of triangle ZBD, is about to be inserted. Stars denote candidate points. Spoke edges from A to the containing polygon ZBD are added. b) The quadrilateral ABCD around suspect edge BD is checked. ABCD can be triangulated in two ways, using diagonals BD or AC, which intersect at point P. c) If BD yields the lowest error, then we have the new triangle ABD and the old triangle CDB. d) If AC has lowest error, then we have the new triangles DAC and BCA, the containing polygon expands to ZBCD, and edges BC and CD become suspect.

If swapping edge BD for edge AC would reduce the global error of the approximation (Figure 5d), then swap the edge to AC, and recurse on the two new suspect edges, BC and CD. When all suspect edges have been tested, it is then necessary to update the candidates for all the triangles in the containing polygon. This straightforward approach requires scan converting most of the triangles in the local neighborhood twice: once to test for swapping and once to find candidates.

A faster alternative is to scan convert once, computing both the global error and the candidate in one pass. This is about twice as fast. To do this, we split the quadrilateral ABCD with its two diagonals into four subtriangles: PDA, PAB, PBC, and PCD, where P is the intersection point of the two diagonals (Figure 5b). This splitting is conceptual; it is not a change to the data structures. As each of the four subtriangles is scan converted, two piecewise-planar approximations are tested. For subtriangle ABP, for example, the planes defined by ABD and BCA are both considered. The other subtriangles have different plane pairs. During scan conversion of each subtriangle, for each of its two planes, the contribution to the triangulation's total error is calculated, and the best candidate point and its error is calculated. After scan conversion, the subtriangles' errors and candidates are combined pairwise to determine the error and candidates for each of the two pairs of triangles: ABD and CDB, versus BCA and DAC. Note that triangle CDB is an old triangle in all cases except the first, mesh initialization, call so its error and candidate have previously been computed, and need not be recomputed.

The algorithm uses all of the previous data structures plus a new one, the *FitPlane*. A *FitPlane* is a temporary data structure that stores an approximation plane and other information. During scan conversion of the four subtriangles, it accumulates information about the error and candidate for a triangle approximated by a plane. Specifically, it contains the coefficients for the planar approximation function *plane*, the candidate's position *candpos* and error *canderr*, the error over the triangle *err*, and a *done* bit recording whether the triangle was previously scanned.

The *Triangle* and *Heap* data structures cache information about candidates and errors that is re-used during data-dependent insertion. A *FitPlane* can be initialized from this information with the subroutine FITPLANE_EXTRACT(*Triangle T*), which also marks the *FitPlane* as *done*. When a new triangle is being tested, the call FITPLANE_INIT(*a, b, c*) will initialize a *FitPlane* to a plane through the three points *a*, *b*, and *c*, with errors set to 0, and *done* = nil. One or more subsequent calls to SCAN_TRIANGLE_DATADEP are made to accumulate error and candidate information in

the *FitPlane*. If this approximation plane turns out to be the best one, the heap is updated and the error and candidate information is saved for later use with a call to SET_CANDIDATE (listed below).

Other routines used below are LEFT_TRIANGLE and RIGHT_TRIANGLE, which return the triangles to the left and the right of a directed edge, respectively. The keyword var marks call-by-reference parameters.

Algorithm IV: Data-Dependent Greedy Insertion:

SET_CANDIDATE(var *Triangle T, FitPlane fit*):
    T.heapptr ← HEAP_CHANGE(*T.heapptr, fit.canderr, T*)
    T.candpos ← *fit.candpos*
    T.err ← *fit.err*

SCAN_POINT(*Point x,* var *FitPlane fit*):
    err ← |$H(x)$ − INTERPOLATE_TO_PLANE(*x, fit.plane*)|
    fit.err ← ERROR_ACCUM(*fit.err, err*)
    if *err* > *fit.err* then
      fit.canderr ← *err*
      fit.candpos ← *x*

SCAN_TRIANGLE_DATADEP(*Point p, Point q, Point r,* var *FitPlane u,* var *FitPlane v*):
    % Scan convert triangle *pqr*, updating error and candidate for planes *u* and *v*.
    % Plane *u* might be nonexistent or already done.
    forall points *x* inside triangle *pqr* do
      if *u* ≠ nil and not *u.done* then
        SCAN_POINT(*x, u*)
      SCAN_POINT(*x, v*)

FIRST_BETTER(float *q1,* float *q2,* float *e1,* float *e2*):
    % Return true iff edge 1 yields better triangulation of a quadrilateral than edge 2,
    % according to shape and fit.
    % *q1* and *q2* are "shape quality", and *e1* and *e2* are fit error of the corresponding triangulations.
    qratio ← MIN(*q1, q2*) / MAX(*q1, q2*)
    % Use shape if shape of one triangulation is much better than other, otherwise use fit.
    if *qratio* ≤ *qthresh* then
      return *(q1 ≥ q2)*   % shape criterion
    else
      return *(e1 ≤ e2)*   % fit error criterion

CHECK_SWAP(*DirectedEdge e, FitPlane abd*):
  % Checks edge *e*, swapping it if that reduces error, updating triangulation and heap.
  % Error and candidate for the triangle to the left of *e* is passed in in *abd*, if available.
  % Points *a*, *b*, *c*, *d*, and *p* are as shown in figure 5b, and *e* is edge from *b* to *d*.
  if *abd* = nil then
    FitPlane abd ← FITPLANE_INIT(*a, b, d*)
  if edge *e* is on perimeter of input grid or quadrilateral *abcd* is concave then
    % Edge *bd* is good and edge *ac* is bad.
    if not *abd.done* then
      SCAN_TRIANGLE_DATADEP(*a, b, d,* nil, *abd*)
    SET_CANDIDATE(LEFT_TRIANGLE(*e*), *abd*)
  else
    % Check whether diagonal *bd* or *ac* has lower error.
    FitPlane cdb ← FITPLANE_EXTRACT(RIGHT_TRIANGLE(*e*))
    FitPlane dac ← FITPLANE_INIT(*d, a, c*)
    FitPlane bca ← FITPLANE_INIT(*b, c, a*)
    SCAN_TRIANGLE_DATADEP(*p, d, a, dac,* %*abd* and convert the four subtriangles
    SCAN_TRIANGLE_DATADEP(*p, a, b, abd, bca*)
    SCAN_TRIANGLE_DATADEP(*p, b, c, cdb, bca*)
    SCAN_TRIANGLE_DATADEP(*p, c, d, cdb, dac*)
    ebd ← ERROR_COMBINE(*abd.err, cdb.err*)
    eac ← ERROR_COMBINE(*dac.err, bca.err*)
    if FIRST_BETTER(SHAPE_QUALITY(*a, b, c, d*), SHAPE_QUALITY(*b, c, d, a*), *ebd, eac*) then
      % keep edge *bd*
      SET_CANDIDATE(LEFT_TRIANGLE(*e*), *abd*)
      if not *cdb.done* then
        SET_CANDIDATE(RIGHT_TRIANGLE(*e*), *cdb*)
    else
      swap edge *e* from *bd* to *ac*
      dac.done ← *bca.done* ← true
      CHECK_SWAP(*DirectedEdge cd, dac*) %recurse
      CHECK_SWAP(*DirectedEdge bc, bca*)

INSERT_DATADEP(*Point a, Triangle T*):
  mark input point at *a* as used
  in triangulation, add spoke edges connecting *a* to vertices of its containing polygon
      (*T* and possibly a neighbor of *T*)
  forall counterclockwise perimeter edges *e* of containing polygon do
    CHECK_SWAP(*e,* nil)

GREEDY_INSERT_DATADEP():
  initialize mesh to two triangles with the height field corners as vertices
  e := (either directed edge along diagonal of initial triangulation)
  CHECK_SWAP(*e,* nil)
  while not GOAL_MET() do
    T ← HEAP_DELETE_MAX()
    INSERT_DATADEP(*T.candpos, T*)

The routines ERROR_ACCUM and ERROR_COMBINE are used to accumulate the error over a subtriangle, and to total the error of a pair of triangles, respectively. These can be defined in various ways. For an L_2 error measure, they should be defined:

```
float ERROR_ACCUM(float accum, float x):
    return accum+x∗x
float ERROR_COMBINE(float err1, float err2):
    return err1+err2
```

and for an L_∞ error measure, they should be defined:

```
float ERROR_ACCUM(float accum, float x):
    return MAX(accum, x)
float ERROR_COMBINE(float err1, float err2):
    return MAX(err1, err2)
```

4.5.1. Combating Slivers

Pure data-dependent triangulation, which makes swapping decisions based exclusively on fit error, will sometimes generate very thin sliver triangles. If the triangles fit the data well, and the surface is being displayed in shaded (not vector) form, then slivers by themselves are not a problem. But sometimes these slivers do not fit the data well, and lead to globally inaccurate approximations. One approach which has been used to combat slivers is a hybrid of data-dependent and Delaunay triangulation [31]. We wished to find a more elegant solution, however.

Our first hypothesis about the cause of the slivers was that narrow quadrilaterals containing few or no input points were never having their diagonals swapped because of the boundary conditions of the inequalities in our code (the case $e1 = e2 = 0$). With either the L_2 or L_∞ error norm described above, triangles containing no input points will have zero error. To address this situation, one can change the error formula to integrate the squared error between the piecewise planar approximation and a bilinear interpolation of the height field grid, instead of simply summing on the grid. This integrated error norm will yield nearly identical results for fat triangles, but it can be quite different for slivers. For a sliver triangle containing no input points, integration will penalize those that deviate from the heights of the input points surrounding the middle of the triangle, while summation will not.

To our surprise, empirical tests disproved this hypothesis, however. When run on both synthetic and real DEM data, pure data-dependent triangulation using an integration error norm yielded no significant improvement over the same algorithm with a summation error norm; it was sometimes a bit better, and sometimes a bit worse. We therefore abandoned the idea of integration in the error norm, and reluctantly adopted a hybrid algorithm.

The pseudocode above implements this hybrid. The procedure SHAPE_QUALITY(a, b, c, d) returns a numerical rating of the shape of the triangles when quadrilateral $abcd$ is split by edge bd. The parameter $qthresh$ is a quality threshold. When set to 0, pure data-dependent triangulation results, when set to 1, pure shape-dependent triangulation results, and when set in between, a hybrid results. If SHAPE_QUALITY returns the minimum angle of the triangles abd and cdb, then this shape-dependent triangulation will in fact be Delaunay triangulation. The hybrid method tended to yield the lowest error approximations overall.

4.5.2. Cost Analysis of Algorithm IV

In a greedy insertion algorithm, the data-dependent triangulation method described above is slower than Delaunay triangulation because it requires about twice as many error recalculations during scan conversion. The asymptotic complexities are identical to algorithm III. Thus, algorithm IV's worst case cost is $O(mn)$ and its expected cost is $O((m+n)\log m)$.
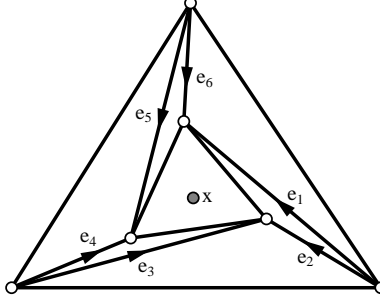
Figure 6: When doing point location on point x in the triangulation above, using Guibas and Stolfi's walking method, if we start at edge e_1, the algorithm loops forever with the sequence of edges shown. Randomization fixes the problem.

4.5.3. A Problem with Location

In the process of testing this algorithm, we discovered that on some of our data-dependent triangulations, Guibas and Stolfi's walking method for point location [13, p. 121], [12], [21] would occasionally loop forever. This was not an implementation error, but a fundamental bug in that algorithm for certain triangulations (see Figure 6). We have never seen this problem arise in algorithms I-III, so we conjecture that it only occurs for non-Delaunay triangulations. Guibas and Stolfi recommended this method for point location in the context of Delaunay triangulation, so perhaps they had never tested it on more general triangulations.

Of course, there are algorithms for point location among m triangles that operate in $O(\log m)$ time [29] that we could use instead, but since the walking method requires only a few lines of code and no preprocessing or extra memory, and it has expected cost of $O(1)$ with the query patterns typical of our algorithms, there is little practical reason to abandon it.

If our conjecture is right, then Guibas and Stolfi's walking method will work fine in algorithms I-III, and since algorithm IV never does point location, this looping bug described will never be exercised there. Nevertheless, for testing purposes it is helpful to have a point location routine that works on general triangulations, so we have modified Guibas and Stolfi's algorithm. We pick the edge to step across at random whenever an arbitrary choice must be made. With this algorithm, the worst case cost of location on a general mesh is an unpleasant $O(\infty)$, as with the unmodified location algorithm, but now this worst case has infinitesimal probability. Its expected cost is still $O(\sqrt{i})$ for random access patterns and $O(1)$ for highly coherent query patterns.

4.6. Extending the Algorithm

So far, we have developed algorithms for simplifying basic height fields, and we have described techniques for making them faster without sacrificing quality. An additional strength of the greedy insertion approach is its flexibility.

First, consider the case in which our data specifies more than just height. For instance, the grid might contain measurements for some material property of the surface such as color, expressed as an RGB triple. Our algorithm can be easily adapted to support such extended height fields. In the simple case we have considered up to now, $H(x, y) = z$ meant that (x, y, z) was a point on the surface. An extended height field produces a tuple of values rather than a simple height; if color were being measured, we might get $H(x, y) = (z, r, g, b)$. We can think of this as sampling a set of

distinct surfaces, one in xyz-space, one in xyr-space, and so on. We see here another reason to reject triangulation schemes that attempt to fit specific surface characteristics; we now have 4 distinct surfaces which need have no features in common. Given data for a generic set of surfaces, we can apply the importance measure to each surface separately and then compute some kind of average of these values. But when we know the precise interpretation of the data (i.e. the values represent height and color), we can construct a more informed measure. Our old measure was simply $|\Delta z|$; the most obvious extension to deal with color is $|\Delta z| + \frac{M}{3}(|\Delta r| + |\Delta g| + |\Delta b|)$. Here, M is the z-range of H; the $\frac{M}{3}$ term scales the total color difference to fit the range of the total height difference (here we assume that color values are between 0 and 1). In order to achieve greater flexibility, we can also add a color emphasis parameter, w, controlling the relative importance of height difference and color difference. The final error formula would be: $(1-w)|\Delta z| + w\frac{M}{3}(|\Delta r| + |\Delta g| + |\Delta b|)$.

To implement these changes, we simply added fields to the height field to record r, g, and b, modified the *FitPlane* to retain planar approximations to these three additional surfaces, and changed the error procedure to use the extended formula above.

These extensions allow our algorithm to be used to simplify terrains with color texture or planar color images [35]. The output of such a simplification is a triangulated surface with linear interpolation of color across each triangle. Such models are ideally suited for hardware-assisted Gouraud shading [9] on most graphics workstations, and are a possible substitute for texture mapping when that is not supported by hardware.

5. Results

We have implemented all four algorithms above. Our combined implementation of algorithms III and IV consists of about 5,200 lines of C++. The incremental Delaunay triangulation module is adapted from Lischinski's code [23].

Figures 7–10 are a demonstration of algorithm III on a digital elevation model (DEM) for the western half of Crater Lake. Figure 7 shows the full DEM dataset (a rectangular grid with each quadrilateral split into two triangles). Our first approximation, shown in Figure 8, uses 0.5% of the points in the original DEM. As you can see, it has defined the major features of the terrain, but is lacking fine details. Next, Figure 9 shows an approximation using 1% of the total points. This approximation contains significantly more detail than the first one. However, it is still clearly different from the original. Finally, Figure 10 is an approximation using 5% of the original points. This model contains most of the features of the original. Obviously, if the viewpoint were moved progressively further from the terrains, the simpler approximations would become steadily harder to differentiate from the original. Thus, we can see that with only a fraction of the original data points, we can build high fidelity approximations. In a multiresolution database, we would produce a series of approximations, for use at varying distances.

Color Figures 23–25 illustrate the application of height field simplification methods to the approximation of planar color images by Gouraud shaded triangles. Figure 24 shows approximation by uniform subsampling as in the "nth-point algorithm", and Figure 25 shows approximation by data-dependent greedy insertion (algorithm IV), both using the same number of vertices. In both cases, the best results (shown) were achieved by low pass filtering the input before approximating. Clearly, greedy insertion yields a much better approximation.
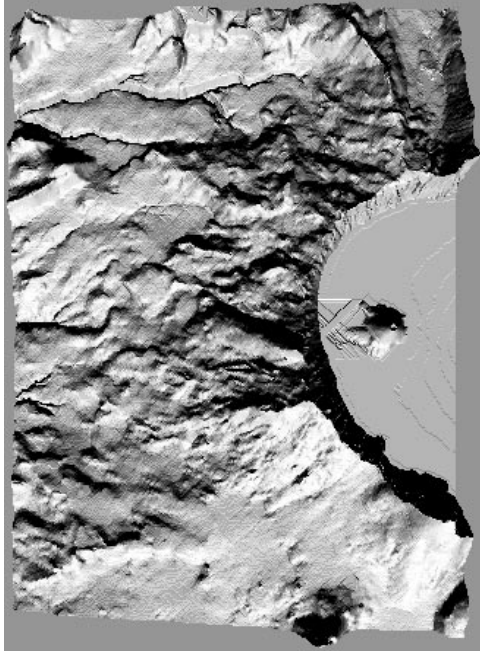
Figure 7: Original DEM data for West end of Crater Lake (154,224 vertices). Note the island in the lake.
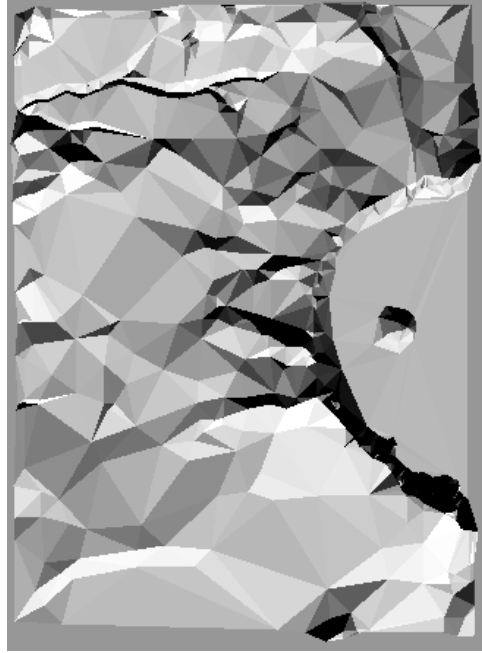
Figure 8: Approximation using 0.5% of the input points, generated by algorithm III (771 vertices).

5.1. Speed of the Algorithms

We have tested the performance of the four incarnations of the simplification algorithm on an SGI Indigo2 with a 150 MHz MIPS R4400 processor and 64 megabytes of main memory. For our tests we have used several digital elevation models (DEMs). They are summarized in Table 4.

Figure 13 shows the running time of algorithm III on the various DEM datasets as a function of points selected in the approximation. In all cases, it was able to select 50,000 points in under one minute. In this and each of the following graphs, n is fixed (although it varies between datasets of different sizes) and the horizontal axis is m. All of the data points in Figure 13 are fit by the

Name	Dimensions	Comments
Ashby	346×452	Ashby Gap, Virginia
Crater	336×459	West half of Crater Lake, Oregon
NTC	$1,024 \times 1,024$	Desert around Mt. Tiefort, California
Ozark	369×462	Ozark, Missouri
West US	$1,024 \times 1,024$	Section of Idaho/Wyoming border

Table 4: DEM datasets used for testing the simplification algorithms.

23
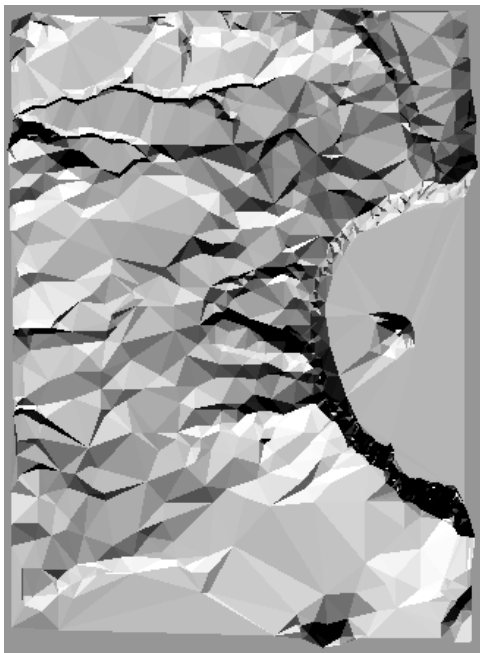
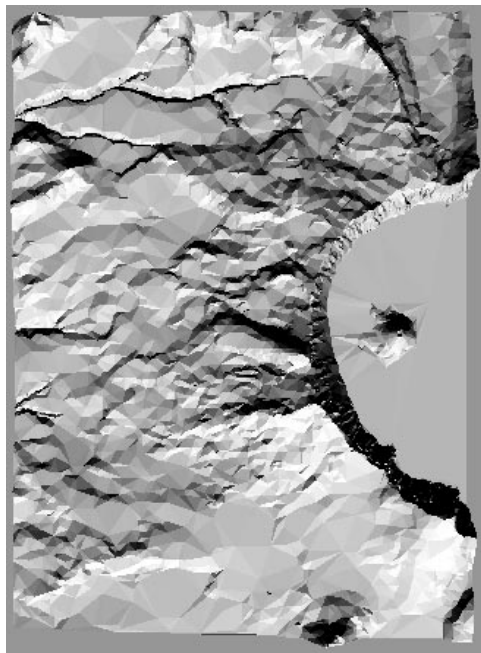Figure 9: Approximation using 1% of the input points, generated by algorithm III (1,542 vertices).

Figure 10: Approximation using 5% of the input points, generated by algorithm III (7,711 vertices).

function

$$\text{time}(m,n) = .000001303\,n\log m - .0000259\,m\log m + .00000326\,n + .000845\,m - 0.178\log m + .1 \text{ sec.}$$

with a maximum error of 1.7 seconds, supporting our $O((m+n)\log m)$ expected cost formula.

Figure 14 compares the running times[6] of algorithms I–III on a 65×65 synthetic terrain. As you can see, the improvement due to our optimizations is dramatic. The running time of algorithm III is dwarfed by the running time of the other two algorithms. This figure also provides another significant point of comparison. In the time it takes algorithm III to select 50,000 points from a $1,024 \times 1,024$ terrain (46 seconds), algorithm I can only manage to select a few hundred points from a 65×65 terrain. These speedups were achieved without sacrificing quality; since algorithms II and III are merely optimizations of algorithm I with no significant change in the points selected or the approximation generated[7].

To provide some insight into the component costs of simplification, we have collected some further performance data in Figures 15 and 16. Figure 15 shows the total number of point interpolations performed as points are selected. Figure 16 outlines the total number of swap operations

---

[6]Timing curves in Figure 14 use relatively unoptimized inner loops. Other timing tests in this paper use inner loops that are over four times faster.

[7]In the case of ties between candidates of equal importance, implementation details might cause a difference in selection order.
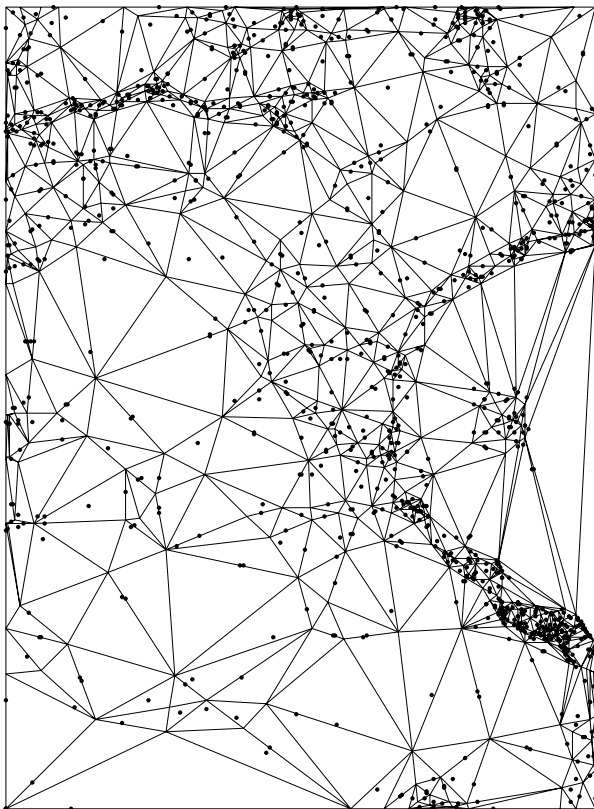
Figure 11: Delaunay mesh for Crater Lake, generated by algorithm III (555 vertices). Candidates are shown with dots. It is interesting to note that most candidates fall near edges.
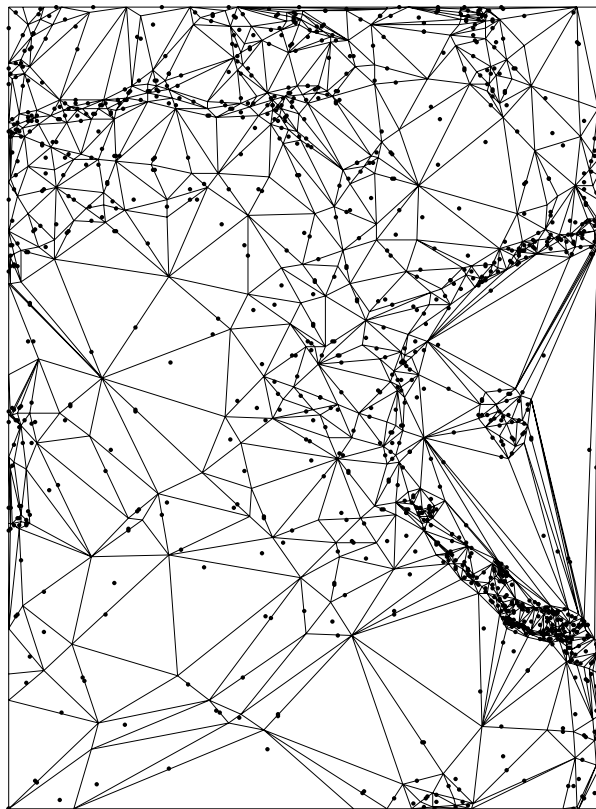

Figure 12: Data-dependent mesh for Crater Lake, generated by algorithm IV (555 vertices).

performed in the heap. These graphs confirm two facts that we intuitively expected. First, the cost of recalculation is very significant in early passes, but it quickly becomes much smaller. In addition, the total cost due to managing the heap grows fairly steadily through time. From our earlier analysis, we concluded that the cost per pass should be $O(\log i)$. However, from looking at this graph, it would seem that the total number of swaps in the heap is growing by a constant number at each pass. Indeed, for most of the shown curves, we can fit very good approximating lines. However, such linear approximations would quickly fail if the fraction of points selected (the ratio m/n) were larger. Heap growth continues until the algorithm begins to run out of unselected input points, at which point the heap shrinks and heap movement decreases as well.

5.2. Memory Use

We now detail the memory requirements of our current implementation. Memory is divided between the height field, the mesh, and the heap. For every point in the height field, we store one 2-byte integer for the z value, and a 1-byte Boolean determining whether this point has been used. Thus,
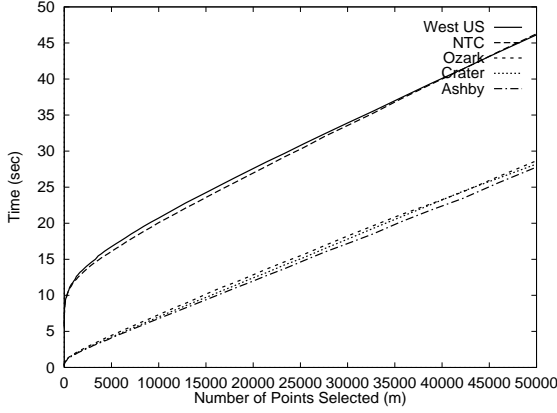
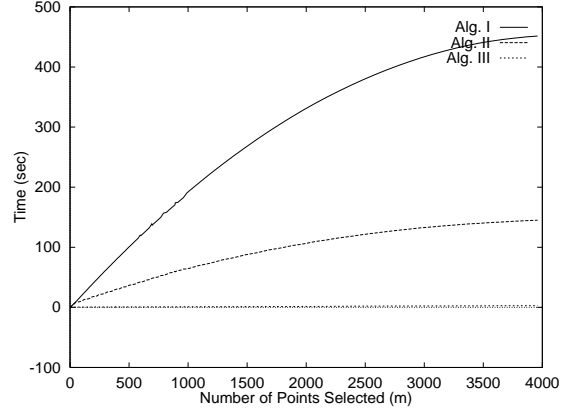Figure 13: Running time of algorithm III on several DEM datasets.

Figure 14: Running time of algorithms I, II, and III on a 65×65 synthetic fractal terrain.

these arrays consume $3n$ bytes. In the mesh, 16 bytes are used to store each vertex's position, 68 bytes are used per edge, and 24 bytes per triangle, so assuming that the number of edges is about $3m$ and the number of triangles is about $2m$, the memory required for a mesh with m vertices is $268m$ bytes. The heap uses 12 bytes per node, and the number of heap nodes is no more than the number of triangles, so heap memory requirements are about $24m$ bytes.

Total memory requirements of the data structures in our implementation are thus $3n + 292m$ bytes. Thus, for example, we estimate that selecting $m = 10,000$ (about 1% of total) points from an $n = 1,024^2$ DEM would require about 6 megabytes of memory.

Our current implementation stores floating point numbers using double precision (8 bytes), and uses the quad-edge data structure to store the mesh, which is less compact than some triangulation data structures, so the program's memory requirements could probably be cut in half if necessary.

5.3. Quality of the Approximations

We believe that the greedy insertion algorithm yields good results on most reasonably smooth height fields. This can be verified both visually and with objective error metrics. Figures 17 and 18 show the RMS and maximum error, respectively, as an approximation for the Crater Lake DEM is built one point at a time. These figures also show the error behavior for some variant insertion policies, but we will ignore these for the moment. While we only show the error curves for a single terrain, we have tested the error behavior on several terrains, and the curves all share the same basic characteristics.

At a coarse level, the RMS error decreases quite rapidly initially and then slowly approaches 0. In the limit as $m \to \infty$, the error of the L_2-optimal triangulation converges as m^{-1} [26], but this empirical data is better fit by the function $m^{-.7}$. In the early phases of the algorithm, the error fluctuates rather chaotically, but it settles into a more stable decline. The non-monotonic shape of this curve suggests why simple hill-climbing algorithms, like the global error measure discussed earlier, might easily fail: if they are unwilling to make a move that temporarily worsens the total error, then they may be incapable of finding the global optimum.
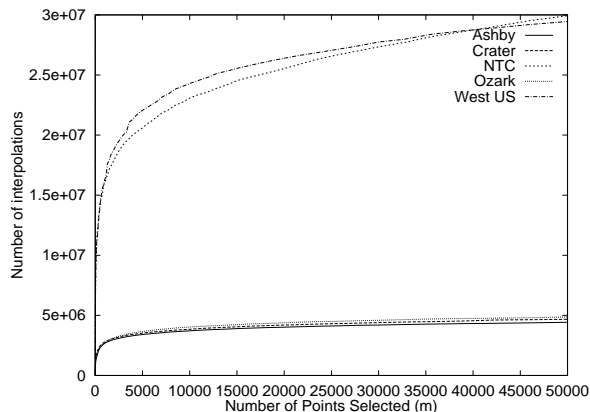
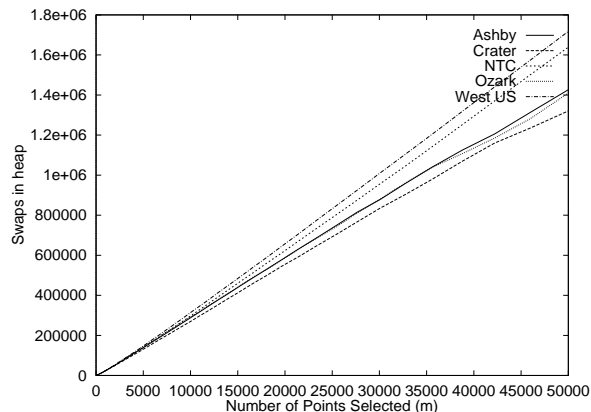Figure 15: Interpolation cost in algorithm III on several DEM datasets.

Figure 16: Number of swaps in the heap as points are selected from the DEM datasets with algorithm III.

For the same dataset, Figure 18 records how the maximum difference between the approximation and the Crater Lake DEM progresses over time; in other words, this is the importance of the point that was selected on each pass. Notice that it is much more chaotic than the total RMS error. Initially, large spikes in the maximum difference correspond to large decreases in RMS error. However, in later passes, significant spikes in the maximum error correspond to only minor alterations in RMS error. In general, we find the RMS error to be a better measure of approximation quality than maximum error, since it is less sensitive to outliers and gives steadier numbers with all algorithms observed.

The hybrid of data-dependent triangulation with shape-dependent triangulation yielded the lowest error overall. For our SHAPE_QUALITY measure, we employed a simple formula which is the product of the areas of the two triangles divided by the product of their approximate diameters. While this does not yield Delaunay triangulation when $qthresh = 1$, we believe the difference is negligible. A shape quality threshold of $qthresh = .5$ gave the best results in most cases. Empirical tests showed that the lowest error approximations resulted when ERROR_ACCUM used the MAX function while ERROR_COMBINE used addition – thus, a combination of L_∞ and L_2 measures.

Delaunay greedy insertion (algorithm III) is compared to data-dependent greedy insertion (algorithm IV) in Figures 19 and 20. The first shows that, for a given number of points, data-dependent triangulation finds a slightly more accurate approximation than Delaunay triangulation. The ratio of data-dependent RMS error to Delaunay RMS error is about .88 for this height field. The second figure shows the time/quality tradeoff very clearly. With either algorithm, as the number of points selected increases, the error decreases while the time cost increases. To achieve a given error threshold, data-dependent greedy insertion takes about 3–4 times as long as Delaunay greedy insertion, but it generates a smaller mesh, which will display faster.

Data-dependent triangulation does dramatically better than Delaunay triangulation on certain surfaces [8]. The optimal case for data-dependent triangulation is a ruled surface with zero curvature in one direction and nonzero curvature in another. Examples are cylinders, cones, and height fields of the form $H(x, y) = f(x) + ay$. On such a surface, if a Delaunay-triangulated approximation
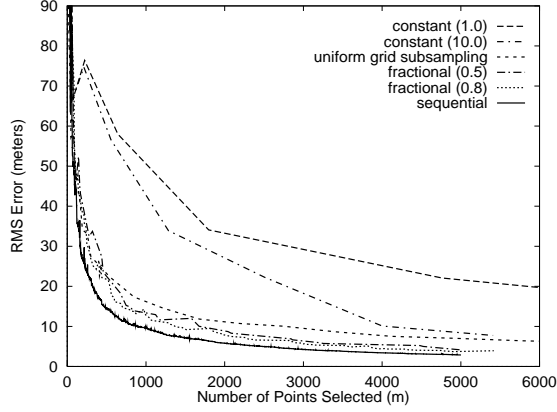
Figure 17: RMS error of approximation as vertices are added to the mesh, for Crater Lake DEM, showing error curves for sequential insertion, fractional threshold parallel insertion with two different fractions α, and constant threshold parallel insertion with two different thresholds ϵ.
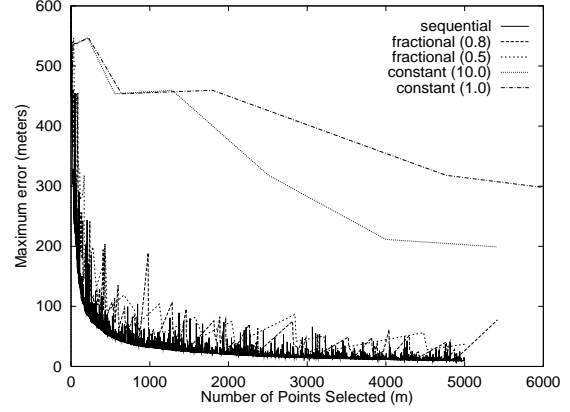
Figure 18: Maximum error of approximation as vertices are added to the mesh, for Crater Lake DEM.

uses m roughly uniformly distributed vertices, then data-dependent triangulation could achieve the same error with about $2\sqrt{m}$ points using sliver triangles that span the rectangular domain.

From our empirical tests, it seems that the surfaces for which data-dependent triangulation excels are statistically uncommon among natural terrains. We conjecture that data-dependent triangulation does not yield significantly higher quality approximations than Delaunay triangulation for natural terrains, in general.

5.4. Sequential versus Parallel Greedy Insertion

In previous work, Puppo *et al.* tested both sequential and parallel greedy insertion and showed statistics that suggest that the latter is better, saying: "...we show the results obtained by the sequential and the parallel algorithm ...Because of the more even refinement of the TIN, which is due to the introduction of many points before the Delaunay optimization, our [parallel] approach needs considerably fewer points to achieve the same level of precision" [30, p. 123].

We tested this claim by comparing our sequential greedy insertion algorithm against two variants of parallel insertion. Both variants select and insert all candidate points p such that $\text{ERROR}(p) \geq \epsilon$, where ϵ is a threshold value. Our implementation of algorithm III contains a data structure holding the candidate for each triangle, so it was easily modified to select and insert more than one candidate per pass.

The first insertion variant, which we call *fractional threshold* parallel insertion, selects all candidate points such that $\text{ERROR}(p) \geq \alpha e_{\max}$, where $e_{\max}$ is the maximum error of all candidates. This is an obvious generalization of sequential insertion, which selects a single point such that $\text{ERROR}(p) = e_{\max}$. Fractional thresholding with $\alpha = 1$ is almost identical to sequential insertion; it differs only in that it may select multiple points with the same error value (this is closely related
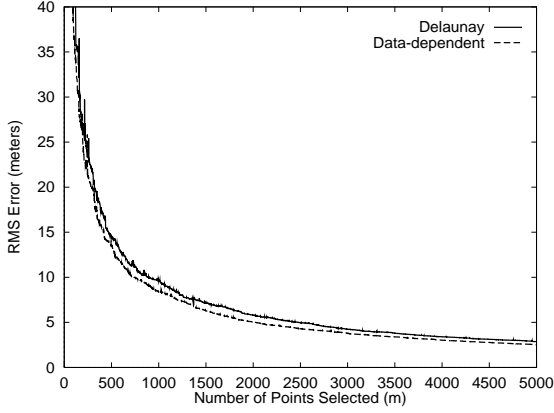
28

Figure 19: RMS error of approximation as vertices are added to the mesh, for Crater Lake DEM, comparing Delaunay triangulation to data-dependent triangulation.
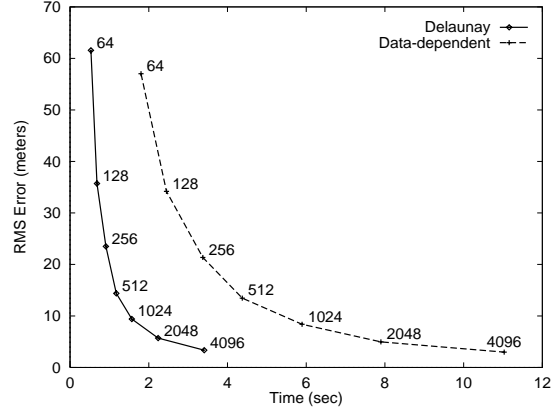
Figure 20: Time versus error plot for Delaunay and data-dependent triangulation on Crater Lake DEM. Data-dependent triangulation is slower, but higher quality. Data points are marked with m, the number of vertices selected.

to the approach of Polis *et al.* [28]). If $\alpha = 0$, fractional thresholding becomes highly aggressive and selects every triangle candidate. Looking at the error graphs in Figures 17 and 18, we can see that as α increases towards 1, the approximations become more accurate and converge to sequential insertion.

The second insertion variant is the rule used by the latter passes of Fowler-Little and by Puppo *et al.* [10, 30]. We call it *constant threshold* parallel insertion. In this case, ϵ is the constant error threshold provided by the user. Thus, on each pass we select and insert all candidate points that do not meet the error tolerance.

Our tests showed constant threshold parallel insertion to be poorer than sequential insertion. The error curves for the constant threshold method in Figures 17 and 18 show it performing much worse than sequential insertion or fractional thresholding. Comparing the meshes in Figures 11 and 21, we can see that the latter is obviously inferior. When an insertion causes a small triangle to be created, it leads to a local change in the density of candidates. With the sequential method, smaller triangles are statistically less likely to have their candidates selected, because they will typically have smaller errors. In the parallel method, if the small triangles' candidate is over threshold, it will be selected, and a snowballing effect can occur, causing excessive subdivision in that area. Even on a simple surface like a paraboloid, which is optimally approximated by a uniform grid, the sequential method is better. On all tests we have run, sequential greedy insertion yields better approximations than parallel greedy insertion.

De Floriani seems to have reached a similar conclusion. While comparing her sequential insertion algorithm to a form of constant thresholding in which the selected points are not limited to one per triangle, she said: "parallel application of such an algorithm by a contemporaneous insertion of all points which have an associated search error greater than the tolerance and belong to the same search region, could lead to the insertion of points which are not meaningful for an improvement
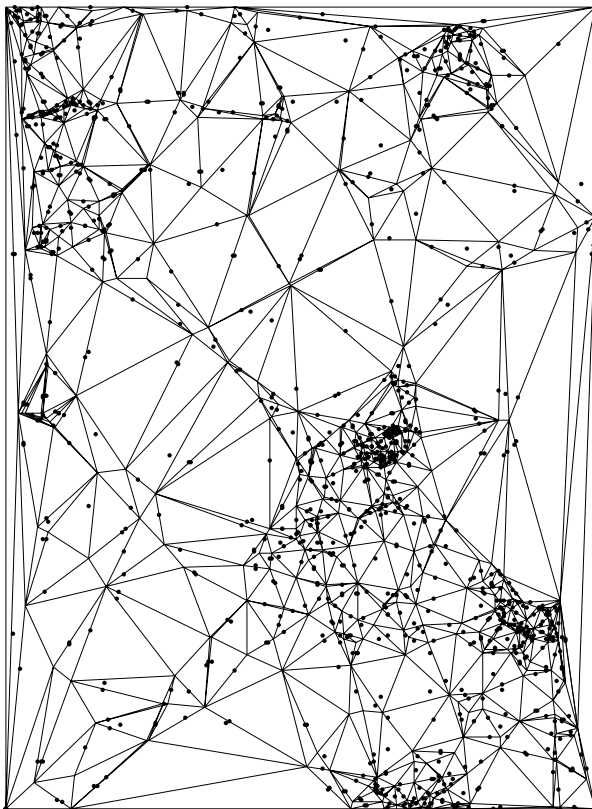
Figure 21: Mesh for Crater Lake using constant threshold parallel insertion, using a variant of algorithm III (555 vertices). Candidates are shown with dots. Note the excessive subdivision near the center and the poor definition of the island.
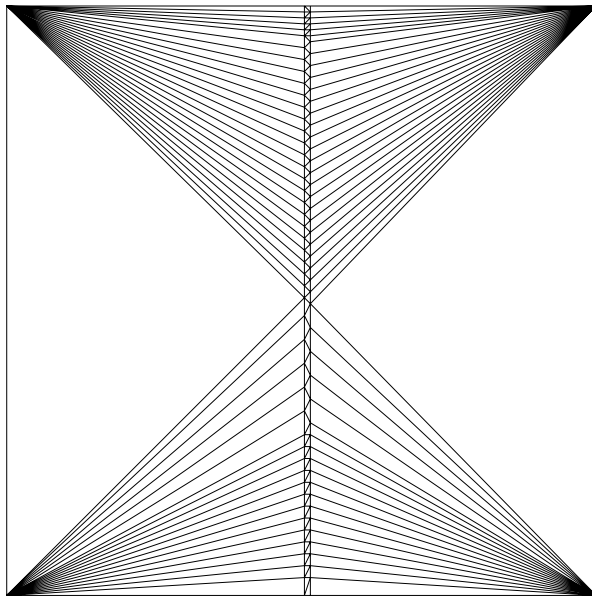
Figure 22: Bad mesh caused by a cliff. Top view of mesh generated by sequential greedy insertion (algorithm III) for a terrain with constant height 0 on the left half of the grid and constant height 1 on the right half. From a 100×100 grid, 99 vertices were selected to achieve zero error; 8 vertices suffice.

in the accuracy of the model" [7, p. 342].

6.   Ideas for Future Research

Our experimentation has suggested several avenues for further research.

Using Extra Grid Information.   The sequential greedy insertion algorithms we have described could easily be generalized to accommodate and exploit additional information about the height field being approximated. For instance, a particular application might wish to guarantee that certain features of a terrain are preserved. It is trivial to preinsert critical points into the approximation mesh. If this is not sufficient, the triangulator can be replaced with a constrained Delaunay triangulator [2], thus allowing arbitrary edges to be preinserted and left untouched by later phases of the simplification process. Ridge lines, valley lines, roads, load module boundaries,

and range data discontinuities [1] are examples of such features. In addition to specifying critical features which will be maintained in the approximation, the user can also be given discretionary control over point selection. The system could be trivially extended to support selective fidelity [28], allowing an importance weight to be assigned to each vertex. Importance values computed at a vertex would be scaled by the specified weight. Weight might also be represented as a function of some sort; for instance, weight might be a function of height or slope. This extension would allow the user to emphasize or de-emphasize certain areas of the height field, and thus gain more direct control over the final approximation.

Speeding Early Passes.   Early passes of our algorithms are slow because they entail scan conversion and recomputation of error for large areas of the height field. This cost can be eliminated if the vertex set is seeded in a hybrid feature/refinement approach, or if exhaustive scan conversion is avoided. The challenge is to speed the algorithm without sacrificing approximation quality. One approach is to choose initial points using variable-window feature selection [18]. Another is to initialize a candidate point to the triangle's centroid, then use a few iterations of hill climbing to move it to the point of locally maximum error [10]. A third approach is to scan convert with subsampling, only examining every kth point in x and y. The relative quality of the approximations resulting from these optimizations is not known.

Combating Slivers.   Pure data-dependent triangulation generates too many slivers. It would be nice to find a more elegant solution to the sliver problem to replace the hybrid algorithm. Our current hypothesis to explain the failure of the integration error norm is that although integration was yielding a better error measure, the resulting improvements were being swamped by the shortsightedness of the greedy insertion algorithm. Sometimes more than one edge swap is required to correct a sliver problem, but our data-dependent greedy insertion algorithm never looks more than one move ahead, so it often gets stuck in local minima.

The Cliff Problem.   The sequential greedy insertion algorithm does not do well when the height field contains a step discontinuity or "cliff". With the greedy insertion algorithm, a linear cliff of length k between two planar surfaces can use up about k vertices, as shown in Figure 22, when, in fact, 4 would suffice. Cliffs similar to this arise when computer vision range data is approximated with this algorithm (this can be seen in the pictures of Schmitt and Chen [34]). This problem is definitely caused by the short-sightedness of greedy insertion. One, somewhat *ad hoc*, solution is to find all cliffs and constrain the triangulation to follow them [1].

Dealing With Noise and High Frequencies.   The greedy insertion algorithms we have described will work on noisy or high frequency data, but they will not do a very good job. There are two causes of this problem. One is the simple-minded selection technique, which picks the point of highest error. Such an approach is very vulnerable to outliers. Finding a better strategy for point selection in the presence of noise appears quite difficult. A second cause is that triangles are not chosen to be the best fit to their enclosed data, but are constrained to interpolate their three vertices. Least squares fitting would solve this latter problem.

A Hybrid Refinement/Decimation Approach.   A technique that might permit better approximations of cliffs and better selection in the presence of noise is to alternate refinement and decimation passes, inserting several vertices with the greedy insertion approach, and then deleting a few vertices that appear the least important, using Lee's drop heuristic approach [22]. Pavlidis employed a similar split-and-merge method for curves [27, p. 181], while Schmitt and Chen used a related method for surfaces [34]. This approach would eliminate the unnecessary vertices from Figure 22, for example. Although such a hybrid of refinement and decimation ideas resembles the

algorithm of Hoppe *et al.* [19], it should be quite a bit faster since we already know how to do many of the steps quickly.

If the least squares approach is taken further, allowing the vertex positions to drift in x and y, as well as z, this would provide an additional mechanism by which the algorithm could correct sub-optimal selections caused by noise or high frequency detail in the height field.

Generalization to Other Geometries. The algorithms presented here could easily be generalized from height field grids to scattered data approximation. That is, the xy projection of the input points need not form a rectangular grid, but could be any finite point set. This change would require each triangle to store a set of points [6, 18, 11]. During re-triangulation, these sets would be merged and split. Instead of scan converting a triangle, one would visit all the points in that triangle's point set.

Generalization of these techniques from piecewise-planar approximations of functions of two variables to curved surface approximations and higher dimensional spaces [15] is fairly straightforward.

Multiresolution Modeling. Further work is needed to build on the algorithms described here to create multiresolution databases for fast terrain rendering. Such a system would need to support division of a huge terrain into blocks, precomputation of multiple levels of detail, adaptive selection of level of detail during display, and blending between levels of detail. Much of this work has already been done by others [28, 20].

Applications in Computer Vision. Finally, these algorithms can be used for the simplification of range data in computer vision. The output data of many stereo and laser range scanners is in the form of a height field or z-buffer in a perspective space, so it can be fed into the algorithms described here with little or no modification. When the triangles output by the algorithms are perspective-transformed to world space, their planarity is preserved, so the approximation in that space is also valid.

Some range scanners acquire data in a cylindrical format, outputting radius as a function of azimuth and height: $r(\theta, z)$. The algorithms here could be modified to generate triangulated approximation to these surfaces, but since the transform between cylindrical space and world space is not a perspective one, nonlinear interpolation would be needed for best results.

As a binary variant of the selective fidelity concept, range data points that are known to be inaccurate can be flagged before being fed into the simplification algorithm, and these points can easily be ignored during vertex selection and error calculation. Our present implementation supports this option. Further work is needed to test the present algorithm's sensitivity to noise and cliffs, and to determine if modification is necessary to deal with these two issues.

7. Summary

In this work we have implemented, optimized, and analyzed the greedy insertion algorithm.

The greedy insertion algorithm is a fast, flexible method that produces high quality approximations. It takes a height field as input and produces a triangulated mesh approximating that height field as output. The algorithm starts with a minimal approximation consisting of two triangles and repeatedly inserts as a vertex in the triangulation the input point with the greatest approximation error. The process is terminated either when a given number of vertices is reached, or when the

error drops below a given error tolerance.

Beginning with a very simple implementation of the greedy insertion algorithm, we optimized it in two ways. First, we exploited the locality of mesh changes, and only recalculated the errors at input points for which the approximation changed, and second, we used a heap to permit the point of highest error to be found more quickly. When approximating an n point grid using an m vertex triangulated mesh, these optimizations sped up the algorithm from an expected time cost of $O(mn)$ to $O((m+n)\log m)$. This speedup is significant in practice as well as theory. For example, we can approximate a 1024×1024 grid to high quality using 1% of its points in about 21 seconds on a 150 MHz processor. The memory requirements of the algorithm are $O(m+n)$. We were able to achieve high speeds and simplify large grids with standard workstations; we did not employ more expensive computers.

We explored several variants of the greedy insertion algorithm in search of the best method for selecting important vertices. The four importance measures examined were: local error, curvature, global error, and products of these. We also tested refinement algorithms, which successively build up a triangulation, against decimation algorithms, which successively simplify it. Our empirical comparisons on curves showed that a multi-pass refinement algorithm utilizing the local error measure, namely, the sequential greedy insertion method, produced the highest quality results.

Delaunay and data-dependent triangulation methods were compared. The latter is capable of higher quality approximations because it chooses the triangulation based on quality of data fit, not on the shape of a triangle's xy projection.

Data-dependent triangulation can be relatively fast. Had we used the straightforward algorithm, data-dependent triangulation would have been many times slower than Delaunay triangulation, since it would scan convert about twice as many input points, doing more work at each point, and it would visit each of these points twice, once for swap testing and once for candidate selection. We described a new, faster data-dependent triangulation algorithm that merges swap testing and candidate selection into one pass, saving a factor of two in cost.

With our implementation, we found that data-dependent triangulation takes about 3–4 times as long as Delaunay triangulation, and yields slightly higher quality on typical terrains. In applications where simplification speed is critical, Delaunay triangulation would be preferred, but if the quality of the approximation is primary, and the height field will be rendered many times after simplification, then the simplification cost is less important, and the data-dependent method is recommended.

We were surprised that data-dependent triangulation did not work better on terrain, since it approximates certain surfaces, such as ruled surfaces, much better than Delaunay triangulation. Perhaps this says something about the isotropy of curvature in natural terrains. Further work is needed to investigate this.

The greedy insertion algorithm is quite flexible. It makes no assumptions that limit its usage to terrains; it is applicable to any height field. In addition, it is easily generalized to extended height fields with material properties such as color. Indeed it can be trivially generalized to arbitrary discrete functions defined over a rectangular domain; examples include the approximation of color raster images by a set of Gouraud shaded polygons, and approximating computer vision range data with triangulated surfaces.

Compared to previous work, our Delaunay greedy insertion algorithm yields nearly identical approximations to those of De Floriani *et al.*, Rippa, and Franklin [7, 31, 11], but from the information available, it appears that our algorithm is the fastest both in theory and in practice.

Part of Heller's adaptive triangular mesh filtering technique is a greedy insertion algorithm

33

employing heaps and local recalculation. That portion of his algorithm appears nearly identical to ours in quality and asymptotic complexity [18, p. 168]. Because the initial pass of his algorithm uses feature selection, we suspect, however, that his could be faster but that our method will produce somewhat higher quality approximations.

We have tested our sequential greedy insertion algorithm against the parallel greedy insertion algorithms of Fowler-Little and Puppo *et al.* [10, 30], and found that sequential greedy insertion yields superior approximations in all cases tested. It appears that the sequential method uses vertices more carefully and leads to less unnecessary subdivision in the mesh.

While the greedy insertion algorithm discussed here is quite fast, and for most terrains it generates high quality approximations, it is far from perfect. It does poorly in the vicinity of cliffs and in the presence of high noise levels or high frequencies, generating approximations that are far from optimal in those cases. Several ideas for improving the algorithm have been proposed here.

Further empirical and theoretical comparisons between methods will be needed to reach a deeper understanding of the surface simplification problem.

Portable C++ code for our Delaunay and data-dependent greedy insertion algorithms (algorithms III and IV) is available by World Wide Web from http://www.cs.cmu.edu/~garland/scape or by anonymous FTP from ftp.cs.cmu.edu in /afs/cs/user/garland/public/scape.

8.   Acknowledgements

9.   References

[1] Xin Chen and Francis Schmitt. Adaptive range data approximation by constrained surface triangulation. In B. Falcidieno and T. Kunii, editors, *Modeling in Computer Graphics: Methods and Applications*, pages 95–113. Springer-Verlag, Berlin, 1993.

[2] L. Paul Chew. Constrained Delaunay triangulations. *Algorithmica*, 4:97–108, 1989.

[3] James H. Clark. Hierarchical geometric models for visible surface algorithms. *CACM*, 19(10):547–554, Oct. 1976.

[4] Thomas H. Cormen, Charles E. Leiserson, and Ronald L. Rivest. *Introduction to Algorithms*. MIT Press, Cambridge, MA, 1990.

[5] Mark de Berg and Katrin Dobrindt. On levels of detail in terrains. In *Proc. 11th Annual ACM Symp. on Computational Geometry*, Vancouver, B.C., June 1995. Also available as Utrecht University tech report UU-CS-1995-12, URL=ftp://ftp.cs.ruu.nl/pub/RUU/CS/techreps/CS-1995/.

[6] Leila De Floriani. A pyramidal data structure for triangle-based surface description. *IEEE Computer Graphics and Applications*, 9(2):67–78, March 1989.

[7] Leila De Floriani, Bianca Falcidieno, and Caterina Pienovi. A Delaunay-based method for surface approximation. In *Eurographics '83*, pages 333–350. Elsevier Science, 1983.

[8] Nira Dyn, David Levin, and Shmuel Rippa. Data dependent triangulations for piecewise linear interpolation. *IMA J. Numer. Anal.*, 10(1):137–154, Jan. 1990.

[9] James D. Foley, Andries van Dam, Steven K. Feiner, and John F. Hughes. *Computer Graphics: Principles and Practice, 2nd ed.* Addison-Wesley, Reading MA, 1990.

[10] Robert J. Fowler and James J. Little. Automatic extraction of irregular network digital terrain models. *Computer Graphics (SIGGRAPH '79 Proc.)*, 13(2):199–207, Aug. 1979.

[11] W. Randolph Franklin. tin.c, 1993. C code, URL=ftp://ftp.cs.rpi.edu/pub/franklin/tin.tar.gz.

[12] P. J. Green and R. Sibson. Computing Dirichlet tesselations in the plane. *The Computer Journal*, 21(2):168–173, 1978.

[13] Leonidas Guibas and Jorge Stolfi. Primitives for the manipulation of general subdivisions and the computation of Voronoi diagrams. *ACM Transactions on Graphics*, 4(2):75–123, 1985.

[14] Leonidas J. Guibas, Donald E. Knuth, and Micha Sharir. Randomized incremental construction of Delaunay and Voronoi diagrams. In *Proc. 17th Intl. Colloq. — Automata, Languages, and Programming*, volume 443 of *Springer-Verlag LNCS*, pages 414–431, Berlin, 1990. Springer-Verlag.

[15] Bernd Hamann and Jiann-Liang Chen. Data point selection for piecewise trilinear approximation. *Computer-Aided Geometric Design*, 11:477–489, 1994.

[16] Paul S. Heckbert and Michael Garland. Multiresolution modeling for fast rendering. In *Proc. Graphics Interface '94*, pages 43–50, Banff, Canada, May 1994. Canadian Inf. Proc. Soc. URL=http://www.cs.cmu.edu/~ph.

[17] Paul S. Heckbert and Michael Garland. Survey of surface approximation algorithms. Technical report, CS Dept., Carnegie Mellon U., 1995. CMU-CS-95-194, URL=http://www.cs.cmu.edu/~garland/scape.

[18] Martin Heller. Triangulation algorithms for adaptive terrain modeling. In *Proc. 4th Intl. Symp. on Spatial Data Handling*, volume 1, pages 163–174, Zürich, 1990.

[19] Hugues Hoppe, Tony DeRose, Tom Duchamp, John McDonald, and Werner Stuetzle. Mesh optimization. In *SIGGRAPH '93 Proc.*, pages 19–26, Aug. 1993.

[20] Michael Jones. Lessons learned from visual simulation. In *SIGGRAPH '94 Course Notes CD-ROM, Course 14: Designing Real-Time Graphics for Entertainment*, pages 39–71. ACM SIGGRAPH, July 1994.

[21] Charles L. Lawson. Software for C^1 surface interpolation. In John R. Rice, editor, *Mathematical Software III*, pages 161–194. Academic Press, NY, 1977. (Proc. of symp., Madison, WI, Mar. 1977).

[22] Jay Lee. A drop heuristic conversion method for extracting irregular network for digital elevation models. In *GIS/LIS '89 Proc.*, volume 1, pages 30–39. American Congress on Surveying and Mapping, Nov. 1989.

[23] Dani Lischinski. Incremental Delaunay triangulation. In Paul Heckbert, editor, *Graphics Gems IV*, pages 47–59. Academic Press, Boston, 1994.

[24] David Marr. *Vision*. Freeman, San Francisco, 1982.

[25] Donald E. McClure and S. C. Shwartz. A method of image representation based on bivariate splines. Technical report, Center for Intelligent Control Systems, MIT, Mar. 1989. CICS-P-113.

[26] Edmond Nadler. Piecewise linear best L_2 approximation on triangulations. In C. K. Chui et al., editors, *Approximation Theory V*, pages 499–502, Boston, 1986. Academic Press.

[27] Theodosios Pavlidis. *Structural Pattern Recognition*. Springer-Verlag, Berlin, 1977.

[28] Michael F. Polis and David M. McKeown, Jr. Issues in iterative TIN generation to support large scale simulations. In *Proc. of Auto-Carto 11 (Eleventh Intl. Symp. on Computer-Assisted Cartography)*, pages 267–277, November 1993. URL=http://www.cs.cmu.edu/~MAPSLab.

[29] Franco P. Preparata and Michael I. Shamos. *Computational Geometry: an Introduction*. Springer-Verlag, New York, NY, 1985.

[30] Enrico Puppo, Larry Davis, Daniel DeMenthon, and Y. Ansel Teng. Parallel terrain triangulation. *Intl. J. of Geographical Information Systems*, 8(2):105–128, 1994.

[31] Shmuel Rippa. Adaptive approximation by piecewise linear polynomials on triangulations of subsets of scattered data. *SIAM J. Sci. Stat. Comput.*, 13(5):1123–1141, Sept. 1992.

[32] Lori Scarlatos. *Spatial Data Representations for Rapid Visualization and Analysis*. PhD thesis, CS Dept, State U. of New York at Stony Brook, 1993.

[33] Lori L. Scarlatos and Theo Pavlidis. Optimizing triangulations by curvature equalization. In *Proc. Visualization '92*, pages 333–339. IEEE Comput. Soc. Press, 1992.

[34] Francis Schmitt and Xin Chen. Fast segmentation of range images into planar regions. In *Conf. on Computer Vision and Pattern Recognition (CVPR '91)*, pages 710–711. IEEE Comp. Soc. Press, June 1991.

[35] David A. Southard. Piecewise planar surface models from sampled data. In N. M. Patrikalakis, editor, *Scientific Visualization of Physical Phenomena*, pages 667–680, Tokyo, 1991. Springer-Verlag.

[36] Michael Spivak. *A Comprehensive Introduction to Differential Geometry*. Publish or Perish, Inc., 1979.

[37] William Welch. *Serious Putty: Topological Design for Variational Curves and Surfaces*. PhD thesis, CS Dept, Carnegie Mellon U., 1995.

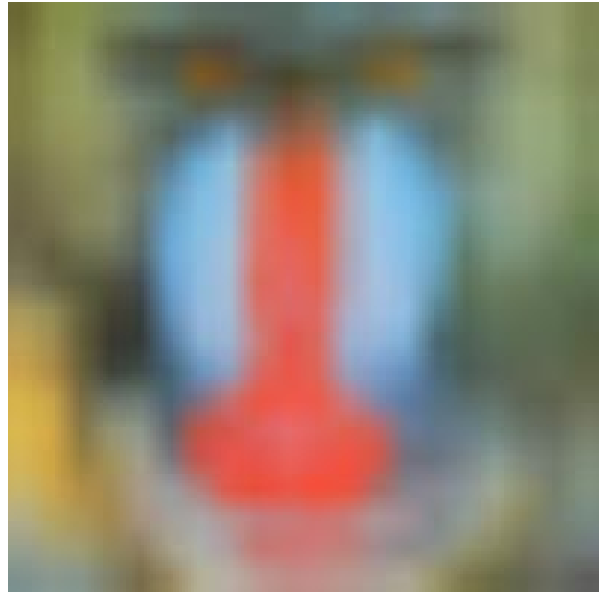Figure 23: Mandrill original, a 200×200 raster image.

Figure 24: Mandrill approximated with Gouraud shaded triangles created by subsampling on a uniform 20×20 grid (400 vertices).
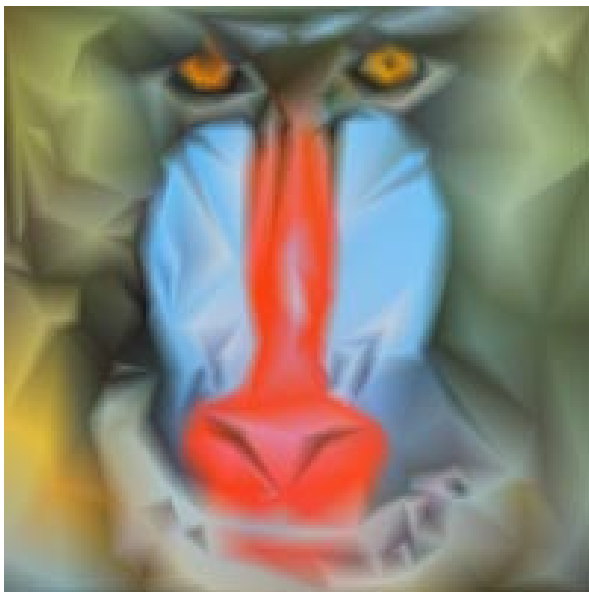

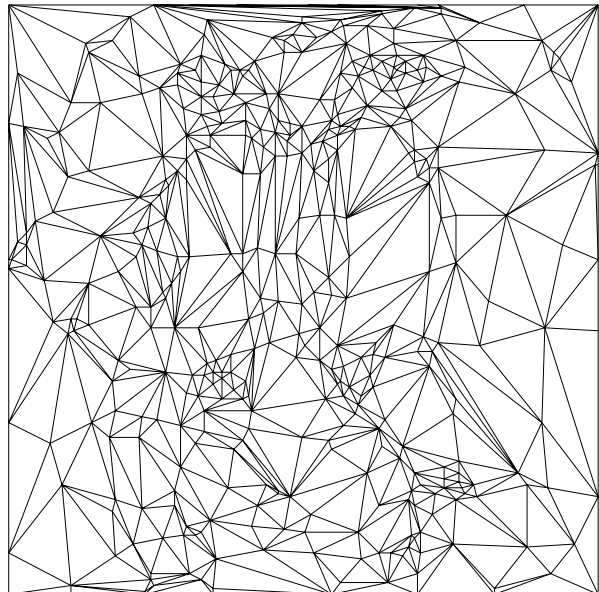Figure 25: Mandrill approximated with Gouraud shaded triangles created by data-dependent greedy insertion (400 vertices).

Figure 26: Mesh for the image to the left.